CONTROL AND ASSESSMENT OF TRANSHUMERAL PROSTHETIC SYSTEM

By

Nasser A. Alshammary

Dissertation

Submitted to the Faculty of the
Graduate School of Vanderbilt University in
partial fulfillment of the requirements
for the degree of

DOCTOR OF PHILOSOPHY

in

Electrical Engineering

May 31, 2017

Nashville, Tennessee

Approved:

Professor Michael Goldfarb, Ph.D.

Professor Xenofon Koutsoukos, Ph.D.

Professor Eric J. Barth, Ph.D.

Professor Richard Alan Peters, Ph.D.

Professor Gerasimos Bastas, M.D., Ph.D.

To my wife, daughter and my mother, who have encouraged me through my life, and supported me through graduate school. I could never have done this work without their belief in me, encouragement and continuous support.

ACKNOWLEDGMENT

There are many people who have helped me throughout my time in the Center for Intelligent Mechatronics, and without whom the work presented here would have been impossible.

Professor Michael Goldfarb, my advisor, has guided me to put my project in the best track and helped solve the challenges I faced in my research. I am thankful for his trust, time and continuous support.

I would also like to thank Profs. Alan Peters, Xenofon, Barth, and Bastas for serving as my committee. I would like to thank King Abdulaziz City for Science and Technology (KACST) who funded my project and my stipend, specifically I'd like to thank Dr. Khalid Aldakkan, a former CIM member who worked as my project principal investigator with KACST, and has provided much support, financial and otherwise, over the course of the project.

I also would like to thank other CIM members who worked on the foundation of my project before I joined, especially Dr. Skyler Dalley and Dr. Daniel Bennett. Dr. Dalley designed the Vanderbilt Multigrasp Hand and developed the Multigrasp Myoelectric Controller which I used in my initial assessment in my project. Dr. Bennet further developed hand design and worked together with me for several years, and had been a great help in designing the coordinated control method for the elbow joint.

I am also thankful to Dr. Brian Lawson who is currently a postdoc at CIM who has helped me machining parts and for his excellent guidance and advises. I also would like to express my deepest gratitude to Don Truex, a research engineer at CIM, who helped designing the electronics boards

in my project and always welling to answer my coding question. Don didn’t hesitate anytime during his busy schedule to utilize his long experience pushing my project forward.

Dr. Jason Mitchell worked on the mechanical design of the transhumeral prosthesis prototype which I used to test different control methods, without a hardware this work would be limited to theoretical concepts.

Last but not least, I would also like to thank all CIM members for the great professional, enjoyable and friendly work environment they created.

TABLE OF CONTENTS

LIST OF FIGURES

Figure Page

LIST OF TABLES

Table Page

CHAPTER 1

INTRODUCTION

This dissertation details the research conducted in the Center for Intelligent Mechatronics (CIM) at Vanderbilt University in collaboration with King Abdulaziz City for Science & Technology (KACST) on the development of a myoelectric transhumeral prosthesis.

The objective of this work is the development of highly functional and intuitive controller for an arm prosthesis that exhibits improved functionality relative to existing traditional transhumeral prostheses control methods, in order to enhance the ability of amputees to perform activities of daily living (ADLs). The work presented in this dissertation utilizes a previously developed a multigrasp prosthetic hand which was presented in several conference and journal publications [1-11]. Specifically, this dissertation explores leveraging recent advances in microelectromechanical systems (MEMS) inertial measurement units (IMUs) in order to develop a controller that enables the simultaneous movement of the anatomical shoulder joint and prosthetic elbow joint, and also enables switching between control of a hand and elbow, and is used in conjunction with electromyogram (EMG) input to provide enhanced whole arm (hand and elbow) control, relative to the traditional sequential control approach which provides one joint control at a time.

This dissertation is organized as follows: this chapter provide an introduction to the field of the upper limb prosthetics. Relevant literature is discussed in Chapter II. Preliminary assessment of a multigrasp myoelectric control approach for use by transhumeral amputees studies are presented in chapter III, which was published in *Engineering in Medicine and Biology Society (EMBC), 2012 Annual International Conference of the IEEE*. Chapter IV presents a novel controller for the coordinated control of a prosthetic elbow and hand using an inertial measurement unit

(IMU) and also an assessment of the presented controller and performance comparison with the traditional control method of transhumeral prosthesis, and was published in *Robotics and Automation (ICRA), 2016 IEEE International Conference on 2016.* An extended analysis of this work has been submitted to *IEEE Transactions on Neural Systems and Rehabilitation Engineering* and is currently in revision. Chapter V describes the implementation and assessment of an IMU-enhanced controller for a transhumeral myoelectric prosthesis and implementation of the controller on a myoelectric transhumeral prosthesis prototype. This work also presents a case study of a single transhumeral amputee subject testing the controller in a series of pick-and-place tasks, in which the subject used the combined IMU/EMG controller, and also a conventional EMG-only controller. The manuscript will be submitted to *IEEE/ASME Transactions on Mechatronics*. Chapter VI summarizes the contribution of this dissertation and discusses recommendations for future work.

1.1 DEMOGRAPHIC AND DEMANDS OF UPPER LIMBS AMPUTEES

The human arm is a complex system that allows us to interact with the surrounding environment and perform our daily needed activities. Several arm configurations can be performed by the human arm with ease, which outperforms even the most sophisticated man-made robotic manipulators. Therefore, losing such a coordinated system will limit the interaction with our environment, affect the body appearance, and may impose social and physical limitations [12].

In 2005, studies indicated that there were approximately 1.6 million people affected by limb loss in the United States, and this number has almost certainly grown in subsequent years. Many of these individuals (35%) had amputations of their upper extremity. The vast majority of amputations are caused by either dysvascular disease, which has a higher incidence in persons 65

years or older (56%), or trauma, which has a higher incidence in persons under 65 (75%). Since approximately 92% of upper extremity amputations are caused by trauma and upper extremity amputations account for approximately 69% of all trauma-related amputations, it follows that the majority of upper limb amputees are most likely under the age of 65 [13, 14]. This means that even though there is a relatively small number of upper extremity amputees (relative to the lower extremity), and far fewer amputees with major (i.e., above wrist) amputations, the population contains a large number of young people who are probably more active and thus might find their lifestyles more drastically impaired by their loss of limb. To replace of the function of the lost limb, amputees turn to prosthetics as alternatives. However, due to the complexity of the replaced limb, the functional limitations of the prosthetic devices limit the benefit. The majority of the amputees rate their prostheses as "fair" or "not acceptable" [15]. Common complaints include poor socket fits, low functionality, and poor appearance [16]. Amputees also desire better control mechanisms that require less visual attention, and the ability to coordinate two or more joints simultaneously [17]. Amputees also desire better control mechanisms that require less visual attention, and the ability to coordinate two or more joints simultaneously [18].

1.2 TRANSHUMERAL PROSTHESIS OVERVIEW

In general, a transhumeral prosthesis is comprised of hand, sometimes referred to as terminal device (TD), an elbow, and possibly a wrist. Transhumeral prostheses can be classified as: cosmetic prostheses, passive prostheses, body powered prostheses or electrically powered prostheses. Cosmetic prostheses are molded from different material like rubber and painted to mimic the shape of the natural human arm, but they are stationary and have no form of control. Instead, they are static and amputees use them for appearance. Passive devices are set in a certain configuration and position (e.g., flexing the elbow or closing the hand) and locked passively by

the use of the other extremity and in the same manner, passive prosthesis are unlocked or by pushing against a surface or object. Even though cosmetic and passive prostheses restore the cosmetic appearance and can appear remarkably life-like and often match the skin tone and contours of the wearer limb, they have no actively moving parts. These devices are the lightest and most simple type of upper extremity prosthesis and can be pre-positioned in specific positions to hold light objects. Many amputees may choose such devices to restore the cosmetic appearance of the arm. However, the gained benefit of these devices is limited to appearance which is not the case in body powered and electrically powered devices.

1.2.1 BODY-POWERED DEVICES

Body-powered devices generally utilizes a split-hook type TD (i.e., hand), where the hook is (typically) maintained in a closed configuration by elastic bands, and is opened via a cable and harness worn by the user. Specifically, movement of the shoulder (typically either scapular abduction or shoulder depression, depending on the type of harness) will generate cable excursion, which in turn opens the split-hook against the tension of elastic bands. This type of configuration is called *voluntary opening* where the TD remains closed until the harness pulled to open the TD. The configuration is called *voluntary closing* where the TD remains open until pulling on the cable occurs to close it. On the other hand, body-powered elbows are controlled by the same cable that operates the TD with an additional attachment or button that operates the elbow lock. When the elbow is unlocked, pulling on the cable will flex (bend) the elbow. When the elbow is locked or fully flexed, pulling on the cable will operate the terminal device. Body powered transhumeral prosthesis is depicted in Fig. 1.

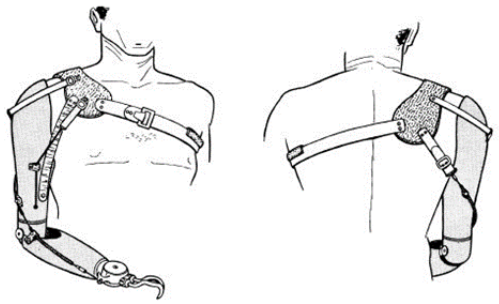

Fig. 1 Body Powered (cable) Transhumeral Prosthesis

This type of prosthesis is environmentally robust, relatively low cost, and offers to the user the benefits of some proprioception and force feedback, in which information regarding the movement and force of the prosthesis (in this case the terminal device) is registered by the shoulder musculature controlling the movement [19].

1.3 ELECTRICALLY-POWERED DEVICES

Electrically-powered prostheses, usually referred to as myoelectric devices, utilizes electric motors for actuation rather than body power (i.e., rather than a harness and cable). Control of the prosthesis is provided by a pair of surface electrodes embedded in the socket, which measure the surface electromyogram (EMG) in the residual limb. Specifically, the opening and closing of the hand or flexion and extension of the elbow, are controlled "directly" via a pair of EMG electrodes, located for a transhumeral amputee on the biceps and triceps, respectively, of the residual upper arm. In the typical control structure, the velocity of opening or closing the hand or flexing/extending the elbow is commanded in proportion to the measured amplitude of the respective EMG electrode. A switching signal, typically a co-contraction (contracting the biceps and triceps momentarily at the same time) is required to select either elbow or hand control, a subsequent co-contraction will cycle the control back to the other component. Myoelectric

prostheses typically have a more anthropomorphic appearance than body powered prostheses, and they do not require shoulder movement or the associated harness to generate motion. However, shoulder movement is indeed required in reaching tasks like in pick-place tasks.

Millstein [20] in 1986 conducted a study comparing the use of myoelectric and body-powered prostheses in upper extremity amputees, and found a greater acceptance rate (transhumeral and transradial) amongst those fit with a myoelectric prosthesis relative to a body-powered type. A study by Stein and Walley [21] in 1983 found that subjects fit with a body-powered prosthesis could perform activities of daily living (ADL's) on average faster than those fit with a myoelectric prosthesis, but that performing the ADL's with the body-powered device required "extreme" or awkward movements of the trunk, and that the body-powered prosthesis was usable in a smaller portion of the upper extremity workspace than the myoelectric device (due to the need for shoulder input).

Body powered prostheses, however, are fundamentally low dexterity devices. That is, the number of control inputs (i.e., cables) is extremely limited, with the large majority of body powered prostheses having one control cable. Despite this, such devices have the potential to provide considerably more functionality, particularly with regard to the ability to control terminal device and elbow. Myoelectric devices on the other hand tend to be characterized by higher cost and less environmental robustness, but do not require a shoulder harness, enable full range of motion about the shoulder, and due to embedded sensing and control, have the potential for increased movement degrees-of-freedom (DOFs) and control sophistication (e.g., can provide assistive coordination). Moreover, in the last decade, advances in motors, microcontrollers, sensors, battery technology and mechatronics in general have enabled the development of multigrasp hands, advanced prosthetic elbow joints and wrist rotators as an improvement on

prosthetic devices [22-26]. Given the functional limitations of body powered devices indicated by [12, 18, 27], and given the potential of the myoelectric devices to enhance functionality, several research prosthetic arms have begun to evolve (e.g. DEKA Arm [26], RIC Arm [25], Parallel Myoelectric prosthesis [28]). In addition to research prototypes, several prosthetic companies (such as i-Limb, RSL Steeper, Otto Bock and Motion Control) have released commercial devices to the amputee community. Therefore, this dissertation focuses on a control approach for a myoelectric transhumeral prosthesis that is intended to enhance functionality through such enhanced control sophistication.

1.4 TRADITIONAL MYOELECTRIC CONTROL METHOD

Most of the current commercially available myoelectric devices utilize a "direct" control approach, in which the measured EMG from an agonist/antagonist pair of muscles is used to command motion of the prosthesis. In the case of a transhumeral prosthesis, surface EMG sites on the biceps and triceps aspects of the residual upper arm are used to open and close or flex and extend, respectively, the myoelectric hand or elbow. In order to minimize continuous contraction of muscles in the upper arm and reduce the cognitive load on the user, such devices are typically velocity controlled, such that the velocity of hand opening (or closing) or elbow flexion (or extension) is proportional to the amplitude of the EMG measured on the biceps and triceps. With a velocity controlled approach, the user need only be concerned with changes in (hand or elbow) position, rather than the position of the hand or elbow. Thus, once the hand is in a given position, the user can leave it there and not have to expend cognitive effort to maintain that given position. This is particularly important given the lack of sensory information conveyed to the user. In this manner, a user can grasp an object (e.g., a bottle of water), flex/ extend the elbow and carry the object around without having to continuously contract the muscles on the on the residual upper

arm, and without having to continuously (visually) monitor the hand and elbow to ensure that the grasp has been maintained. Rather, once grasped, the user need only perform a subsequent muscle contraction when wanting to release the grasped object or to adjust the elbow position. In such control method, the user can switch the control from the hand to the elbow (or vice versa) by contracting both agonist/antagonist muscles (biceps and triceps) of the residual limb where the pair of EMG electrodes affixed, simultaneously for a short period of time. Alternating control between the joints forces the user to control the joints of the arm in a sequential manner (i.e. one joint at a time) which is not intuitive in relative to the way healthy arm is being controlled. The healthy arm is controlled in a coordinated fashion and requires less cognitive effort. In addition, adding an additional joint to the arm prosthesis (e.g. wrist joint) will presumably increase the cognitive effort using such control method. This is attributed to the limited control inputs to the arm prosthesis which are the surface EMG. As indicated by [16, 17, 27, 29] amputees are not satisfied with their devices, particular due to lack of functionality and intuitiveness. In addition, amputees would like to have more joints (e.g., a wrist) with much visual attention and cognitive load [29, 30]. With fewer inputs to control more joints, new control strategies are required to provide a transhumeral amputee with control of a limb that feels intuitive and natural. Several research efforts addressing this problem have been conducted, which are briefly highlighted in Chapter II of this dissertation.

CHAPTER 2

BACKGROUND AND RELATED WORK

The problem with the use of direct surface EMG to control a prosthesis is that, like the body-powered devices, the number of control channels is severely limited. Commercial devices typically incorporate measurement at two EMG sites, which provides a single (bidirectional) control command to the prosthesis. In the case of a multi-joint prosthesis (e.g., a transhumeral myoelectric prosthesis with an elbow and hand), the single control channel (consisting of the combined biceps and triceps EMG) is switched between elbow and hand control, such that only one is being controlled at any given time.

Although not yet implemented in commercial devices, considerable research has been conducted in the control of myoelectric prostheses via pattern recognition approaches. Pattern recognition approaches offer the potential of simultaneously controlling a high number of degrees-of-motion in a coordinated fashion from a lower number of command inputs in a largely intuitive manner. For example, such an approach could be used to control a hand capable of eight grasp patterns from two agonist/antagonist pairs of EMG electrodes (e.g., from four surface electrodes, such as on the dorsal/ventral and lateral/medial aspects of the forearm). Another Example in [31], such an approach could be used to perform hand open and close, pronation and supination of the wrist and extension and flexion of the elbow. In such an approach, the controller considers windows of EMG information (as opposed to single samples), and based on the pattern of information contained in the window, the controller infers the intent of the user to perform a given motion or grasp posture. Recent, representative examples of such work, incorporating various pattern classification techniques to classify a number of postures and motions for transradial and

transhumeral control from surface EMG measurements for upper limb myoelectric prostheses, for example, see [32-34].

Though EMG pattern classification methods show promise, they also entail some implementation challenges and limitations that hinder their use in commercial prostheses. First, they provide a quasi-real-time (as opposed to real-time) control. The amount of latency in pattern classification depends upon several factors, including the number of EMG sites, the number of pattern classes (or grasp patterns) being recognized, and the desired accuracy of classification. A recent survey of EMG pattern recognition methods indicates decision latencies between 50 ms and 900 ms, depending on the number of inputs, number of classes, desired accuracy, and structure of the classifier [35]. The low end of that bracket (i.e., 50 ms) is unlikely to be an impediment to real-time control, although the high end of the bracket (i.e., 900 ms) would likely impede the natural, real-time interaction with the prosthesis. Another drawback of classical pattern recognition approaches, which is arguably more fundamental, is the inability to move proportionally within a grasp posture or between grasp postures. For example, a pattern classification approach can provide either the pointing posture or the cylinder grasp, but in general cannot provide for the proportional position of the index finger between the two postures. Similarly, controlling the elbow using pattern recognition will lack the proportionality in controlling the elbow position. In addition, even more EMG channels are required in the case of transhumeral amputation which in return will increase the latency in the pattern classification.

The pattern recognition approach presents a fundamental trade-off between the number of classes, the classification "bandwidth" and the accuracy of classification. That is, increasing one will fundamentally lower the other two. Therefore, a large number of pattern classes will entail either low classification bandwidth (i.e., a long classification latency) and/or a low classification

accuracy (i.e., a high incidence of incorrect classifications). Finally, a significant limitation of pattern-based approaches is that the output (i.e., the classification) is highly dependent upon the consistency of the input. In the case of surface EMG, a large number of factors contribute to inconsistency in the EMG input, including movement of the electrodes relative to the underlying muscle, which can be caused by changes in the posture of (the intact joints on) the affected limb (which is exacerbated in biarticular muscles) and movement of the socket (and thus the electrodes) relative to the underlying musculature. Due to these factors, the measured EMG patterns characteristic of a certain grasp posture or elbow control can vary significantly between a configuration in which the elbow (or shoulder) on the affected limb is fully flexed or fully extended. Note that if the position of the intact elbow (and shoulder) could be measured, this effect could be cancelled in the controller, but measurement of shoulder and/or elbow angles is not likely a feasible solution in a commercial product. In addition, since only one class can be selected in one decision, the control of the prosthesis will still be sequential control, in other words, a switch signal still needed to switch the control to other joint.

The absence of clear EMG sites on an amputee's residual limb is a problem in generally any control method involves EMG (e.g. in the case of high level transhumeral amputation or shoulder disarticulation), where the EMG signals required by the algorithms can be difficult or impossible to obtain, but it is even more problematic with pattern recognition control method, since so many more signals are required. In this case, a targeted muscle reinnervation (TMR), which is a surgical operation needed to create additional EMG sites, may improve EMG sites. TMR is a method by which a spare muscle (the target muscle e.g. chest muscle) of an amputated patient is denervated (its original nerves cut and/or de-activated), then reinnervated with residual nerves of the amputated limb. The resultant EMG signals of the targeted muscle now represent the motor

commands to the missing limb, and are used to drive a myoelectric prosthetic device [36, 37]. Although the signals obtained through this method have been shown to be effective and efficient enough to drive the prosthesis, the method requires an invasive surgery.

Direct control approaches used in traditional control methods (e.g., sequential control) offer real-time proportional control and are not highly sensitive to EMG variation, and thus are used in commercially available devices, but as previously discussed cannot provide simultaneous or coordinated control of multi-joint devices (e.g., arm prosthesis with hand and elbow). Therefore, this dissertation describes a novel control method that uses the direct control approach but coordinates the control between the arm joints.

2.1 PRIOR WORK ON THE TRANSHUMERAL PROSTHESIS

Work on the transhumeral prosthesis started with creating a multigrasp hand prosthesis for transradial amputees. Most of the work done prior to the research detailed in this dissertation focuses on the development of a myoelectric multigrasp hand and myoelectric controller which are referred to as the Vanderbilt Multigrasp (VMG) hand and Multigrasp Myoelectric Controller (MMC), respectively. The VMG and MMC were both used in this work. Mainly, the hand was utilized as a terminal device.

2.1.1 VANDERBILT MULTIGRASP HAND (VMG)

VMG is an anthropomorphic prosthetic hand that incorporates four motor units in a unique configuration to explicitly provide both precision and conformal grasp capability. The hand is a self-contained system with an embedded control system located in the palm of the hand as depicted

in Fig. 2. The overall mass of the hand with the embedded system is 546 g. The VMG hand was designed and assessed previously as indicated in [7, 8, 10, 11].

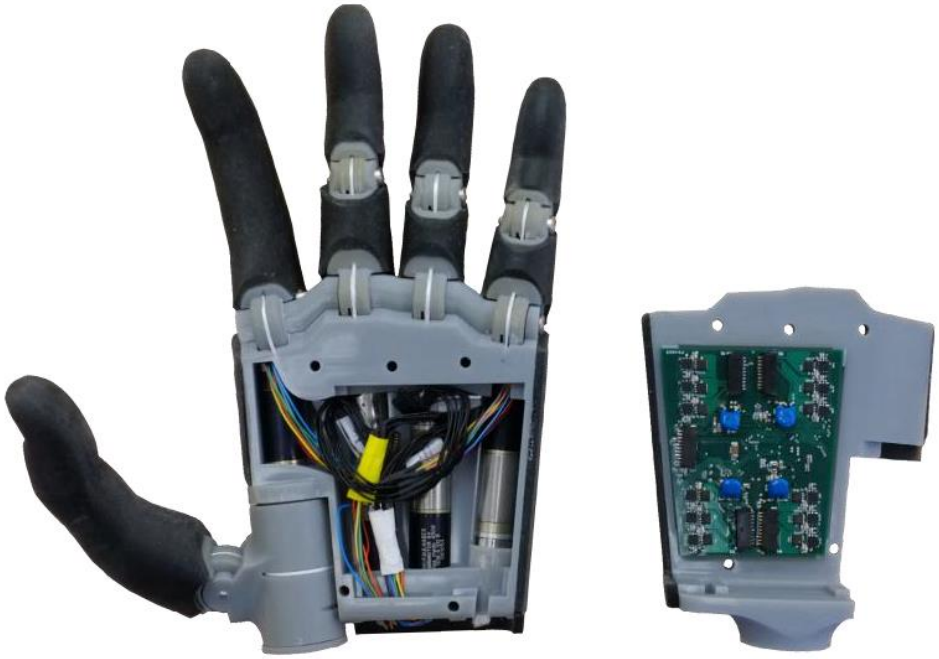

Fig. 2 VMG with the embedded control system

2.1.2 MULTIGRASP MYOELECTRIC CONTROLLER (MMC)

The Multigrasp Myoelectric Controller (MMC) was developed alongside the VMG previously in order to provide intuitive access to the full functionality of a multigrasp prosthetic hand with only the standard 2-site EMG signals [5]. These electrodes provide two control signals that typically correspond to an “open” and “close” command for a single degrees of freedom (DOF) prosthesis. The MMC uses these two signals, along with tendon displacement and force measurements to navigate through a state machine where each state represent a certain hand posture. The MMC was used in this work along with the VMG in assessment of a transhumeral prosthesis which will be explained later in this dissertation.

CHAPTER 3

ASSESSMeNT OF A MULTIGRASP MYOELECTRIC CONTROL APPROACH FOR USE BY TRANSHUMERAL AMPUTEES

The VMG assessed previously for the use of transradial amputees (i.e. EMG placed on anterior and posterior muscles of the forearm) [5]. Hence, the previously developed hand controller for the use of a transradial amputee has been utilized and modified to be used for a transhumeral amputee. The aim of this work was to experimentally assess the ability of a non-amputee subjects to control a hand prosthesis using biceps and triceps muscles instead of forearm muscles. This experiment was performed using a virtual environment and the efficacy of the system has been demonstrated in which the performance of the controller maintaining certain postures has been compared to the performance of the native hand. This work is not the main contribution, however, it's mainly an experiment using a previous work and modify it to fit transhumeral needs. The outcomes of this preliminary assessment of the MMC for use by transhumeral amputees was published in Engineering in Medicine and Biology Society (EMBC), 2012 Annual International Conference of the IEEE studies are presented in this chapter.

3.1 ABSTRACT

The authors have previously developed a multigrasp myoelectric controller, and assessed the ability of healthy subjects to control the configuration of a multigrasp hand prosthesis using musculature on the anterior and posterior aspects of the fore-arm, as would be representative of controller use by a transradial amputee population. In this paper, the authors conduct a similar study, this time to assess the capability of a transhumeral amputee to control a multigrasp hand from residual musculature on the upper arm. Specifically, experiments are conducted on five

healthy subjects, comparing their ability to obtain one of seven hand postures in a virtual prosthesis from EMG measurement of the respective biceps and triceps musculature. The ability to control the virtual hand prosthesis is compared with their ability to do so with their intact hand, as measured by a dataglove. Results indicate an average transition time using the EMG controller on the biceps and triceps of 1.86 seconds, relative to 0.82 seconds with the dataglove.

3.2 INTRODUCTION

As of 2005, there were approximately 41,000 persons living in the United States with major (i.e., excluding loss of fingers) upper limb amputations [13]. Extrapolating from a recent sampling of amputees [12], the two most common levels of major upper limb amputation are the transradial and transhumeral levels, each of which constitute approximately one third of the total upper extremity amputee population. After suffering limb loss, upper extremity amputees generally have two options in prosthesis types for functional replacement of the hand, which are either a body-powered or a myoelectric type. A highly constraining factor in both types of prostheses is the limited number of control inputs with which the user can control the hand prosthesis (or terminal device). Specifically, whether the control input is a body-powered cable or a myoelectric signal, hand prostheses have traditionally been limited to a single control channel, which is typically used to open and close either a split hook (in the body-powered case) or a single degree-of-freedom hand (in the myoelectric case).

Recent technological advances (i.e., the power density of rare-earth magnet brushless motors, the energy density of light metal batteries, the enhanced computational capability of microcontrollers, etc.) have brought to the near horizon the possibility of multigrasp hand prostheses, which are able to provide to the amputee a number of hand postures and grasps. For a

recent survey of several emerging multigrasp prostheses, see [38]. Despite the emergence of such devices, the enhanced functionality they offer is not useful to the amputee without a multigrasp control interface that offers intuitive, effective, and reliable access to the multiple grasps and postures they can provide.

A number of approaches to multigrasp prosthesis control, based on the measurement of surface electromyogram (EMG) as the primary control signal, have been proposed. These fall largely into two categories, which are pattern recognition approaches (e.g., see [39-42]), and hierarchical approaches (e.g., see [43-48]). The authors have developed and previously published a hierarchical multigrasp hand prosthesis control approach, called Multigrasp Myoelectric Control (MMC) [49]. In that paper, the authors focused on the ability of a transradial amputee to control a multigrasp hand prosthesis via two surface EMG electrodes, one on the anterior and posterior aspects, respectively, of the user's forearm. Note, again, that transradial amputees constitute approximately one third of the total upper extremity amputee population.

In this paper, the authors conduct a similar study, but instead of focusing on the efficacy of the approach for transradial amputees, the authors focus on the efficacy of the approach for transhumeral amputees. As previously mentioned, like the transradial amputee population, the transhumeral amputee population constitutes approximately one third of the total upper extremity amputee population. The control method is similar for both populations, although rather than utilizing one electrode site on each of the anterior and posterior aspects of the forearm, respectively, as is the case for transradial amputees, a transhumeral amputee will utilize surface EMG sites on the biceps and triceps muscles, respectively. Such musculature is obviously further removed from operation of the native hand, and thus the authors intent in conducting this study was to assess the extent to which EMG of the upper arm musculature provided effective control of

a multigrasp prosthesis. As such, in this paper, the authors present the results of a study (on five healthy subjects) indicating the ability to control a multigrasp prosthesis from the upper arm, and compare those results to the capability to do the same with the native hand, and to the capability to control from electrode sites on the forearm.

3.3 MULTIGRASP MYOELECTRIC CONTROL

The MMC method involves an event driven finite-state machine that transitions between a finite set of fixed postures (states), where the future state of the prosthesis is determined by the current state and electromyogram (EMG) input to the state machine. This structure is illustrated in Fig. 3. In this work, the MMC control method was modified to better address transhumeral amputations. That is, musculature on the upper arm, as opposed to the lower arm, has been utilized. Specifically, contraction of the biceps muscle (flexion) is associated with upward movement in the state chart, while contraction of the triceps muscle (extension) is associated with downward movement in the state chart. Furthermore, the co-contraction event has been replaced with a double extension action to transition between the opposition and reposition states (which are associated with movement of the thumb). The double extension consists of fully extending the prosthesis within the opposition (or reposition) state, relaxing, and extending again to initiate automatic reposition (or opposition) of the thumb. To this end, the muscle relaxation time has been accounted for in this implementation by determining the relaxation period for each subject during the signal conditioning process. This preserves co-contraction for possible multiplexing between hand and elbow functions, and eliminates the necessity of performing co-contraction during hand motions.

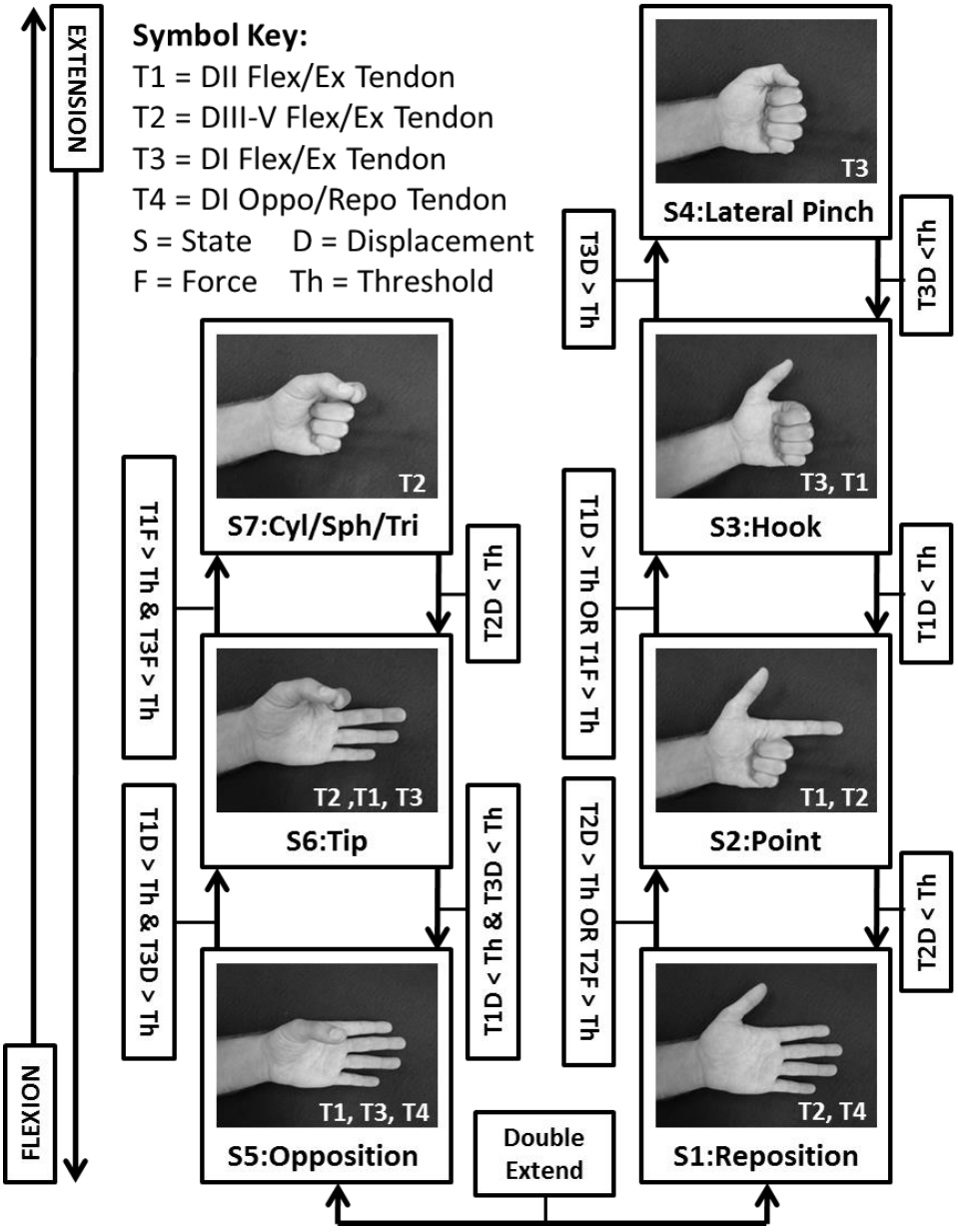

Fig. 3 The Multigrasp Myoelectric Control State Chart. The structure of the MMC finite-state machine. The states are comprised of different hand postures. Transitions from state to state depend on EMG thresholds, and double extension detection logic. Contraction of the biceps is associated with upward movement in the state chart. Contraction of the triceps is associated with downward movement in the state chart. Double extension initiates an automated toggling motion between the opposition and reposition states.

3.4 METHODS

Five non-amputee volunteers, aged 20-30 years, participated in this study. Each volunteer underwent six trials which involved controlling a virtual prosthesis to achieve a series of randomized target postures. In the first six trials, this was done using a dataglove to capture the motion of the native hand. This was followed by six other trials where the MMC was used to control the virtual prosthesis through a similar set of random postures. In this way, the performance of the MMC could be compared to that of the native hand. The time between an individual subject's trials ranged from one to four days with an overall experimental completion period of forty five days. This study was approved by the Vanderbilt University Internal Review Board.

3.4.1 VIRTUAL PROSTHESIS

The virtual prosthesis model developed in [49] was implemented in this study to evaluate the performance of the native hand and the MMC. This model uses a virtual prosthesis which is displayed on a computer screen and controlled by the subject using either the native hand (via a dataglove) or by MMC (via EMG). A virtual ghost (an overlaid duplicate of the virtual prosthesis) is used to display target postures for the user to acquire with the virtual prosthesis.

3.4.2 DATAGLOVE

In order to evaluate the ability of the native hand to obtain preset postures with the virtual prosthesis, a dataglove was used to obtain temporal and spatial data for later comparison with MMC. Specifically, the dataglove captured flexion/extension of the index and middle fingers, as well as flexion/extension and opposition/reposition of the thumb, using variable resistance bend sensors. In the virtual prosthesis, motion of the ring and little fingers was coupled to that of the

middle finger, allowing the achievement of all target postures. Dataglove details may be found in [49].

3.4.3 EMG

To obtain surface EMG data, two Ag/AgCl electrodes (Myotronics, Inc.) were affixed to the subject's skin after each EMG site was sanitized with alcohol pads. The electrodes were positioned over the subject's biceps and triceps muscle bellies (in parallel to the muscle fibers) with a reference electrode positioned proximal to the elbow. These positions were marked for consistent placement between subsequent trials. The output signals of the electrodes were then preamplified (K=100) and low pass filtered (f_c = 500 Hz) near the electrode sites using custom analog circuitry. The signals were then passed to Simulink Real Time Windows Target using a Humusoft MF624 data acquisition card where they were digitally high-pass filtered (f_c = 50 Hz) and rectified. The signals were then digitally low-pass filtered (f_c=5 Hz) to obtain velocity references for the MMC.

3.5 EXPERIMENTAL PROCEDURE

As mentioned above, each trial consisted of achieving random sequences of target postures. The target postures coincide with the MMC states (reposition, point, hook, lateral pinch, opposition, tip and cylindrical). When a new target posture is displayed, the subject manipulates the virtual prosthesis using either the dataglove or the MMC. For the dataglove this manipulation consists of movement of the native hand. For the MMC this consists of isometric contraction of the biceps or triceps muscle (where the subject grasps a rigid handle to isolate movement of the arm). When the virtual prosthesis closely matches the target posture (±25% range of motion) the virtual ghost disappears indicating that the target posture has been achieved. To be considered successful, a target posture must be held for 3 seconds. A new target posture is displayed after

successfully achieving a target posture, or if the target posture is not achieved within five seconds. If five seconds pass without achievement of the target posture the transition is considered a failure, and a new posture is displayed. The time it takes for the subject to achieve a target posture is recorded and defined in this study to be the *transition time*. The percentage of successful target postures achieved in less than five seconds is defined in this study to be the *transition completion rate*. Note that the transition times in this study are influenced by intrinsic biological factors such as visual, cognitive, neural, and muscular delays.

Each subject was given a period of up to 15 minutes to get accustomed to the operation of the dataglove and MMC before performing the experimental trials. Each trial lasted approximately 10 minutes. Note that there are a total of 42 possible transitions among the MMC states (i.e., from any of the seven states, there are six other possible states to which the user can transition). During a trial, each transition type is presented three times, resulting in a total of 126 transitions, with each posture appearing 18 times.

3.6 RESULTS AND DISCUSSION

3.6.1 PERFORMANCE TRENDS

From Fig. 4 it can be seen that, in general, median transition times decreased with subsequent trials. This trend is presumably a result of subject learning over time. After the third trial, the median transition times for both the dataglove and the MMC fell within 10% of their respective means, indicating decreased improvement and minimal gain in the repetition of trials. For this reason, the final three trials were used to compile the data reported herein.

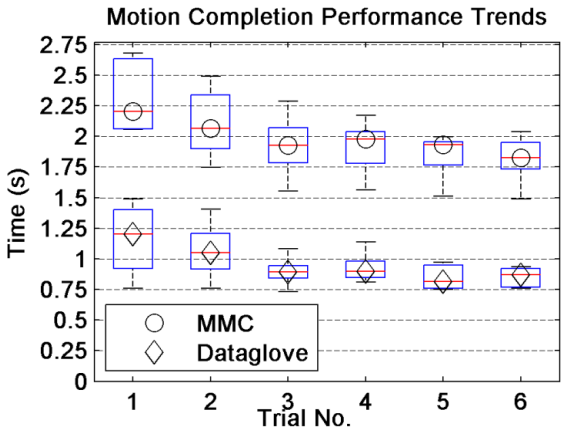

Fig. 4. Median motion completion times for each trial, where each box encompasses the 25th to 75th percentiles for that trial and control method. Whiskers extend to the minimum and maximum recorded times.

3.6.2 TRANSITION TIME

The average transition times for the dataglove (native hand) and the MMC (EMG) trials for each transition type are shown in Table I and Table II, respectively. The standard deviations are noted in parentheses. The average overall transition times (the average time to go from any one posture, to any other) for the dataglove and the MMC were 0.82 seconds (standard deviation of 0.23 seconds) and 1.86 seconds (standard deviation of 0.75 seconds). The difference in these times may be attributed to two primary factors. First, the topography of the state chart dictates that the transition time between postures will be proportional to the distance between them (see Fig. 3.). Second, transitions which require opposition or reposition of the thumb (and therefore, the performance of the double extend action) will necessarily incorporate the muscle relaxation time of the subject, and increase transition times accordingly. Also, variations in relaxation time from subject to subject will lead to increased deviation in transition times for the MMC. In these experiments, the average muscle relaxation time was found to be 0.50 seconds, with a standard

deviation of 0.25 seconds. The average overall transition times and relaxation times for each subject may be found in Table III.

Table I Average Transition Times for All Subjects Using the Native Hand (Dataglove)

		Target Posture						
		Lateral	Hook	Point	Reposition	Opposition	Tip	Cylindrical
Original Posture	Lateral		0.59 (0.26)	0.65 (0.22)	0.68 (0.22)	0.84 (0.50)	1.12 (0.73)	0.82 (0.69)
	Hook	0.55 (0.18)		0.60 (0.18)	0.68 (0.38)	0.89 (0.50)	1.20 (0.73)	0.73 (0.38)
	Point	1.70 (0.34)	0.51 (0.16)		0.65 (0.19)	0.78 (0.29)	1.25 (0.73)	0.83 (0.38)
	Reposition	0.87 (0.32)	0.59 (0.23)	0.73 (0.32)		0.64 (0.28)	1.13 (0.73)	0.85 (0.39)
	Opposition	0.75 (0.27)	0.81 (0.38)	0.82 (0.34)	0.62 (0.25)		1.12 (0.73)	1.13 (0.45)
	Tip	0.72 (0.22)	0.69 (0.39)	0.71 (0.22)	0.79 (0.38)	0.81 (0.30)		0.90 (0.50)
	Cylindrical	0.69 (0.26)	0.72 (0.42)	0.67 (0.25)	0.69 (0.23)	0.96 (0.58)	1.08 (0.73)	

Table II Average Transition Times for All Subjects Using MMC (EMG)

		Target Posture						
		Lateral	Hook	Point	Reposition	Opposition	Tip	Cylindrical
Original Posture	Lateral		1.07 (0.43)	1.31 (0.63)	1.24 (0.19)	1.89 (0.31)	2.65 (0.66)	2.93 (0.52)
	Hook	0.83 (0.20)		0.98 (0.31)	1.04 (0.24)	1.71 (0.45)	2.39 (0.59)	2.63 (0.45)
	Point	2.23 (0.97)	0.99 (0.29)		0.73 (0.2)	1.46 (0.4)	2.23 (0.55)	2.65 (0.62)
	Reposition	1.71 (0.55)	1.42 (0.28)	1.31 (0.44)		1.57 (0.64)	2.34 (0.49)	2.50 (0.40)
	Opposition	3.00 (0.52)	2.91 (0.62)	2.51 (0.53)	1.52 (0.45)		1.24 (0.64)	1.31 (0.25)
	Tip	2.87 (0.56)	2.84 (0.74)	2.42 (0.50)	1.60 (0.43)	0.63 (0.16)		0.98 (0.34)
	Cylindrical	3.10 (0.64)	2.89 (0.48)	2.60 (0.45)	1.63 (0.18)	1.71 (0.28)	1.02 (0.35)	

Table III Average Transition Time and Relaxation Time for Each Subject Using MMC

Subject	Transition Times (seconds)	Relaxation Times (seconds)
HS 1	1.94	0.70
HS 2	1.92	0.38
HS 3	1.84	0.54
HS 4	1.52	0.49
HS 5	2.10	0.41
Average	1.86	0.50

In a previous study, which investigated the use of MMC for transradial amputees [49], the dataglove and MMC transition times were found to be 0.81 seconds (standard deviation of 0.14 seconds) and 1.49 seconds (standard deviation of 0.15 seconds). Note that the transition times in the previous study do not include muscle relaxation time because muscle relaxation (double extension) was not required to transition among the opposition and reposition states. Note, furthermore, that 24 of the 42 transitions in the state chart require opposition or reposition, while 18 of the 42 transitions do not. Therefore, the results of the previous study can be adjusted to arrive at a theoretical estimate of the average overall transition time, if double extension had been utilized, by adding the average muscle relaxation time to the 24 transitions which require opposition or reposition. This is illustrated in the equation (1) below:

$$\left[(1.49\ s)\left(\frac{18}{42}\right)\right] + \left[(1.49\ s + 0.50\ s)\left(\frac{24}{42}\right)\right] = 1.78 \qquad (1)$$

By doing this, it can be seen that the transition times reported in the previous and current study are comparable. Specifically, dataglove transition times for the previous and current study were 0.81 and 0.82 seconds, respectively. The MMC transition times for the previous and current study were 1.78 (as adjusted to reflect the use of double extension) and 1.82 seconds, respectively.

3.6.3 TRANSITION COMPLETION RATE

The transition completion rates for the dataglove and the MMC in this study were found to be 99.2% and 99.3%, respectively. These results indicate that the reported transition times are accurate regardless of whether or not the 5 second cutoff time is considered. These results are also consistent with the transition completion rates reported in [49], indicating that MMC control is dependable at both the transhumeral and transradial level.

3.7 CONCLUSION

This paper presents a version of a previously published multigrasp myoelectric controller which has been modified for use by transhumeral amputees, and investigates the ability of a person to control a multigrasp hand prosthesis from musculature in the upper arm (i.e., from the biceps and triceps muscles). Also, the MMC approach used in this paper utilized double extension to transition between the opposition and reposition states, preserving co-contraction for the future development of multifunction prostheses. The study of five healthy subjects indicates that on average the subjects were able to control the multigrasp capability of the virtual prosthesis using musculature in the upper arm essentially as well as subjects in a previous study were able to control the prosthesis with the musculature in their forearm. The study therefore indicates that the use of the MMC method should apply equally as well to either the transradial or transhumeral levels of amputation.

CHAPTER 4

SYNERGISTIC ELBOW CONTROL FOR A MYOELECTRIC TRANSHUMERAL PROSTHESIS

After the successful assessment of the MMC for transhumeral use, the goal of this project was to design an intuitive coordinated controller as we move up the arm and include more joint. The primary goal of the work described in this chapter was to create a transhumeral prosthesis coordinated controller that would coordinate the control between the controlled components (i.e. hand and elbow control). This goal was achieved by leveraging recent advances in MEMS, specifically, Inertia Measurement Unit (IMU), in order develop a controller that enables the simultaneous movement of the anatomical shoulder joint and prosthetic elbow joint, and also enables switching between control of a hand and elbow, and is used in conjunction with EMG input to provide enhanced whole arm (hand and elbow) control, relative to the traditional sequential control approach. This work was published in *Robotics and Automation (ICRA), 2016 IEEE International Conference on 2016,* and extended analysis of this work has been submitted to *IEEE Transactions on Neural Systems and Rehabilitation Engineering* and is currently in review.

In addition to the published work, the coordinated controller design went through several iterative stages before converging to its final version.

The main contribution to this dissertation is the design and assessment of the coordinated controller. Following the manuscript of the currently in review paper is an addendum discussing the design iterations of the coordinated controller, investigating the experience gained from each controller and how they led to the final version of the coordinated controller.

4.1 ABSTRACT

This paper presents a control approach for a myoelectric transhumeral prostheses, specifically consisting of a myoelectric elbow and terminal device, which supplements a typical two-site EMG input with inertial measurement of arm motion to facilitate prosthesis control. The inertial measurement enables measurement of upper arm motion and is employed to 1) provide synergistic movement between the prosthetic elbow joint and intact shoulder joint, and 2) to switch control between the myoelectric elbow and hand. The objective of the control approach is to reduce the control burden on the amputee user. In order to assess the prospective efficacy of the control method, experiments were conducted on six healthy subjects who performed a series of pick-and-place tasks within a virtual environment. The assessments compared the time required to complete the pick-and-place tasks using the proposed coordinated control approach, with the time required using a sequential control approach (i.e., the conventional approach used in commercial devices). Results of these assessments indicate that subjects on average completed the pick-and-place tasks 32% faster with the coordinated control approach, relative to the conventional sequential EMG method, with no difference in compensatory torso motion.

4.2 INTRODUCTION

It is well known that upper extremity prostheses fall short of expectations of the patient population. Surveys of upper extremity amputees indicate that less than half regularly use their prosthetic arms [12, 27], largely due to functional limitations. Similar surveys report a desire for devices with improved functionality and more intuitive and coordinated control [18]. Two major types of arm prostheses exist – body-powered and myoelectric types. The former offer advantages of relatively low-cost, high environmental robustness, and the ability to relay proprioceptive and

force information to the user [15]. Such devices also require the user to wear a shoulder harness, however, and precludes full range of motion about the shoulder (e.g., preclude use of the prosthesis while reaching overhead). Myoelectric devices tend to be characterized by higher cost and less environmental robustness, but do not require a shoulder harness, enable full range of motion about the shoulder, and due to embedded sensing and control, have the potential for increased movement degrees-of-freedom (DOFs) and control sophistication (e.g., can provide assistive coordination). Given the functional limitations indicated by [12, 18, 27], and given the potential of the latter to enhance functionality, this paper focuses on a control approach for a myoelectric transhumeral prosthesis that is intended to enhance functionality through such enhanced control sophistication.

A myoelectric transhumeral prosthesis typically consists of the combination of a myoelectric hand and elbow. The conventional method for control of this type of myoelectric prosthesis (i.e., the method employed in commercial devices) incorporates a two-site EMG interface, in which a pair of EMG electrodes is placed over the biceps and triceps brachii muscle groups, respectively. The filtered and rectified signals measured by the agonist/antagonist pair of EMG electrodes collectively provide a single (bidirectional) control input to the prosthesis. As such, the user has only a single control input with which to control the two components (i.e., the hand and elbow) of the prosthesis. This limitation is addressed by multiplexing the single (bidirectional) myoelectric control signal between the myoelectric elbow joint and hand, where the multiplexing function is typically performed via a brief muscular co-contraction of the biceps and triceps muscles. Although simple and robust, this “sequential” control approach is considerably less efficient than the simultaneous joint movement characteristic of arm motions in healthy individuals. Further, the sequential method becomes increasingly inefficient with additional myoelectric degrees-of-freedom (DOFs) in the arm (e.g., powered wrist DOFs or multigrasp hands).

It is well known that arm movement in healthy individuals is characterized by the simultaneous movement of multiple joints. A control method that enables such simultaneous (or coordinated) movement of multiple arm joints could presumably increase the efficiency with which amputees with transhumeral prostheses perform activities of daily living (ADLs). One approach to providing coordinated control of multiple joints is to leverage known movement synergies between the (intact) shoulder and (prosthetic) elbow joints. Such synergies have been characterized in biomechanical research studies [19, 50-56]. Among these, Popovic et al. proposed to leverage shoulder-elbow joint synergies during reaching tasks to facilitate control of functional electrical stimulation (FES) in patients with tetraplegia[19, 52-56]. In their work, experiments were performed with healthy subjects to characterize the functional synergies between shoulders and elbow angular velocities during reaching movements. Based on data from these experiments, the resulting synergies were modeled using a proportional relationship between the joint angular velocities, where the constant of proportionality between the two was determined to be a function of the initial and final arm configurations [19, 54]. The authors subsequently further characterized shoulder and elbow joint synergies using radial basis function neural network models, additionally included synergies between the shoulder and forearm pronation/supination[30], and also incorporated these synergies into a "proximal segment controls distal segments" control method for control of FES to facilitate reaching in persons with tetraplegia.

Kaliki et al. also proposed to use the measured orientation of the upper arm to predict distal arm posture for control of neuroprostheses (i.e., FES) and myoelectric transhumeral prostheses [50, 51]. In their research, Kaliki et al. also conducted experiments using healthy subjects to characterize the functional synergies between shoulder angle (i.e., abduction/adduction, flexion/extension, and internal/external rotation), elbow flexion/extension, and forearm

pronation/supination (i.e., wrist rotation) during multiple reaching movements, and additionally included consideration of shoulder location. In their research, the authors used artificial neural networks (ANNs) to construct (i.e., train) three models of arm synergies, and subsequently to characterize the validity of the models via the coefficient of determination (R^2 value). The authors' second model, which is of direct relevance to the work presented here, utilized shoulder location and angle as input, and elbow angle as output, and was characterized by an average R^2 value of 0.85, indicating a strong correlation between the ANN model and the kinematic shoulder/elbow synergy during reaching movements. Based on their results, the authors report that "it is clear [that shoulder angles can be used] to adequately predict the elbow angle for reaching movements in a large three-dimensional extra-personal space" [51].

Although [51] suggest the applicability of their work to transhumeral myoelectric prostheses, the paper is focused on modeling rather than control. Recently, Lauretti et al. [57] proposed a coordinated controller for a transhumeral prosthesis that leverages arm joint synergies similar to those experimentally characterized in the aforementioned studies. Specifically, the controller employs a pair of inertial measurement units (IMUs) on the trunk and residual limb, respectively, to provide a measure of shoulder flexion/extension and shoulder ab/adduction, and combines these measures with a two-site EMG interface, such that a sustained co-contraction of the EMG couples shoulder flexion/extension with elbow flexion/extension and wrist rotation with shoulder ab/adduction. In the absence of sustained co-contraction, EMG control is switched to the hand, and the elbow and wrist are immobilized. The authors implement their controller using healthy subjects in a virtual environment, and show improved completion times of the virtual tasks with the coordinated controller relative to a sequential control approach.

Like the work presented in [57], this paper proposes a control method for a transhumeral myoelectric prosthesis that also leverages the existence of shoulder/elbow synergies. The authors hypothesize that such a control method can enable faster performance of ADLs, specifically those involving reaching, relative to existing sequential EMG controllers. Since movement of the elbow is coordinated with movement of the residual limb (i.e., intact shoulder movement), the authors refer to the method as synergistic or coordinated control. The authors note, however, that the notion of coordination is specifically between the user and prosthesis, as opposed to the coordination of multiple joint motion within the prosthesis.

The control method proposed here is similar to that reported in [57] (which was apparently concurrently developed) in that it also employs a kinematic synergy between shoulder flexion/extension and elbow flexion/extension. The control method, however, is different in at least three major respects. First, the method proposed here modulates the gain between the shoulder and elbow during movement using differential EMG. Second, EMG is not used to switch between elbow and hand control. Rather, the control is switched between the elbow and hand via the IMU, which detects when the hand is moving or stationary, relative to an inertial reference frame, and switches control accordingly. And third, although less fundamental, the method employs a single IMU located on the forearm of the prosthesis (rather than two on the body).

The proposed control approach was implemented on a virtual prosthesis within a virtual environment, and the efficacy of the proposed control approach was assessed in a series of experiments on healthy subjects who conducted reaching tasks within the virtual environment, specifically comparing the ability of subjects to complete reaching tasks using the coordinated controller, relative to their ability to do so using a conventional sequential controller.

4.3 CONTROL METHODS

As previously described, the conventional control approach for the control of a myoelectric transhumeral prosthesis with a myoelectric elbow and hand from a two-site EMG interface (i.e., EMG from biceps and triceps sites) is referred to herein as a sequential control approach. This section first briefly describes and defines this sequential control method, then describes the proposed coordinated control approach. Both the conventional (i.e., sequential) and coordinated control approaches utilize a standard two-site EMG electrode interface, corresponding to one electrode over the biceps muscle group, and one over the triceps. Both controllers also incorporate identical (and standard) signal conditioning of the EMG measurements (subsequently described).

4.3.1 SEQUENTIAL CONTROL APPROACH

The sequential controller employs a standard control structure for control of the hand and elbow joints. Namely, control of either the elbow or hand is selected at any given time by a short-duration co-contraction of both EMG inputs, which toggles the control to one of the two components. The component not being controlled assumes a locked state. .When a component is under EMG control, the differential measurement of the two-site EMG is used to generate an angular velocity command, such that the user contracts the residual limb musculature to induce movement, and relaxes limb musculature to maintain the current configuration. Thus, if e_1 and e_2 represent the filtered and rectified EMG from the biceps and triceps muscles, respectively, the angular velocity reference (or command) for the selected, or active, component is given by:

$$\omega_{emg} = \begin{cases} k_1 e_1 & if\ e_1 \geq e_2 \\ -k_2 e_2 & otherwise \end{cases} \quad (2)$$

where k_1 and k_2 are normalizing gains, typically chosen to provide nominal symmetry of movement (i.e., similar angular velocity responses) in response to similar contractile efforts. Typical signal conditioning such as hysteresis and a dead band around an EMG noise floor are incorporated to facilitate well-behaved, deliberate control. A finite state machine (FSM) depicting the sequential control structure for a typical transhumeral prosthesis is shown in Fig. 5.

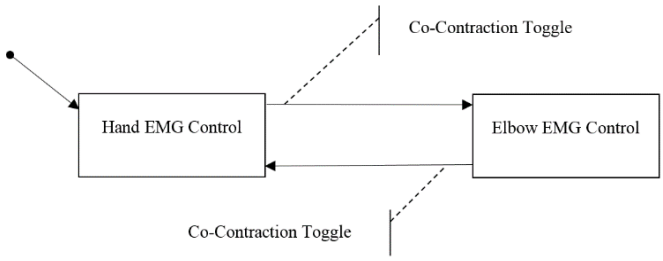

Fig. 5. FSM of sequential elbow/hand control structure

4.3.2 SYNERGISTIC OR COORDINATED CONTROLLER

A. Joint Synergy Approach

This paper proposes a controller that leverages kinematic synergies between the intact shoulder joint and prosthetic elbow joint, particularly during reaching movements, patterned loosely after those experimentally characterized and modelled in [19, 50-54], with the intent of improving the control and functionality of transhumeral myoelectric prostheses. Although the precise form of the models proposed in previous studies were not incorporated as derived in those works for the control method here, the authors note that doing so could be an interesting extension of this work, particularly with regard to potential improvements or refinements associated with three-dimensional mapping of shoulder to elbow joint synergies, and also with regard to the potential to exploit synergies between the intact shoulder and prosthetic wrist joints (which were not considered here). In an effort to start an exploration of the extent to which such models may

offer value in the control of a transhumeral prosthesis, the authors incorporate here a relatively simple model of shoulder/elbow kinematic synergy, similar to the one described in [53, 54], specifically between the shoulder elbow angular velocity and the component of shoulder angular velocity that is collinear with it. As a ball-and-socket joint, the shoulder will in general have three components of angular velocity, while as a hinge joint, the elbow will have one. The method proposed here utilizes as input only the component of shoulder angular velocity collinear with the elbow angular velocity vector, and as such, when referenced hereafter, the term "shoulder angular velocity" refers exclusively to this component of the shoulder angular velocity (i.e., the component associated with shoulder flexion/extension). As described in [53, 54], the synergistic relationship between the shoulder and elbow angular velocities can be approximated as a single-valued nonlinear function, which can be reduced to a linear relationship within a given reaching motion, where the constant of proportionality is a function of the start and endpoints of the reaching motion. Such a model has two problems, however, for practical realization for the control of a transhumeral prosthesis. First, as pointed out in the paper in which it was presented, one cannot in general know the endpoint of the movement during the movement (i.e., the model is causal), and as such the synergistic model cannot be exactly known in real time. Second, although the arm frequently performs reaching tasks, it also performs a variety of other activities, and as such, an invariant algebraic relationship between these joints would likely interfere with other arm functions.

In order to address both these issues in a practical manner, the authors propose the use of a proportional relationship between shoulder and elbow angular velocities, as is described in [53, 54], but unlike the model used there, the constant of proportionality (between joint velocities) can be modulated by the user by superimposing EMG command from the two-site EMG interface onto the nominal linear model of shoulder/elbow synergy. In this manner, a user can selectively

leverage the shoulder/elbow synergy that naturally exists during reaching movements, but can additionally modulate the strength of that synergy for a given task, or can override it completely via superposition of EMG, when necessary or desired for a given task. As such, motion of the myoelectric elbow is governed by the weighted combination of two inputs from the user: shoulder angular velocity and differential EMG, both of which drive elbow angular velocity in a proportional manner.

B. Two Control Inputs: EMG and IMU

It should be noted that the method proposed here actually utilizes upper arm angular velocity, rather than shoulder angular velocity, since the former can be directly measured from the prosthesis without the need for any instrumentation outside of the myoelectric prosthesis. The two quantities are approximately the same in the case that the torso angular velocity is small, relative to upper arm angular velocity. Specifically, upper arm angular velocity is measured in real time in the proposed control approach using an inertial measurement unit (IMU). Given the recent availability, compactness, and low cost of microelectromechanical systems (MEMS) based 6-axis (and 9-axis) inertial measurement units, upper arm motion is straightforwardly measured by mounting a MEMS IMU on the transhumeral prosthesis. Note that an IMU located on the forearm of a transhumeral prosthesis can, when combined with measurement of the prosthetic elbow angle, provide real-time measurement of the three-dimensional orientation of the upper arm. Since the control approach described here reproduces only the synergy between the collinear components of shoulder and elbow angular velocity, the controller requires only the addition of a single-axis gyroscope, aligned with its measurement axis collinear with the axis of the elbow. Thus, for the proposed coordinated controller, a standard two-site EMG interface is supplemented solely with measurement from a single-axis gyroscope, the combination of which provides elbow and hand control. This approach

is aligned with a recent opinion paper in which the authors advocated for the fusion of other sensor information with EMG in order to improve the control of upper extremity prostheses [58].

C. Controller Equations

Given the above description, the coordinated controller is thus a straightforward modification of the standard elbow controller. Specifically, the EMG component of the commanded elbow angular velocity is proportional to the differential EMG measurement, as given in (2). The synergistic component (i.e., reaching component) of the elbow angular velocity is proportional to the measured shoulder angular velocity:

$$\omega_{sy} = k_3 \omega_{ua} \tag{3}$$

where ω_{sy} is the synergistic component of the elbow angular velocity command, k_3 is a coupling coefficient, and ω_{ua} is the measured upper arm angular velocity, which as previously stated, can be assumed to be the shoulder angular velocity when the angular velocity of the torso is small. Note that, if this assumption is not true, the synergy thus becomes one between the upper arm angular velocity and elbow angular velocity, rather than strictly between the shoulder and elbow. The commanded elbow angular velocity is the superposition of the EMG and synergy components of angular velocity, given by:

$$\omega_{eb} = \omega_{sy} + k_4 \omega_{emg} \tag{4}$$

where ω_{eb} is the superposed elbow angular velocity command and k_4 is a weighting factor between the two components of elbow angular velocity command. Thus, the coordinated controller is in implementation a relatively simple modification of the conventional EMG elbow controller. Like the standard sequential controller, the coordinated controller is intended to control only one

myoelectric component (i.e., elbow or hand) at any given time, and thus the control must similarly be switched between the elbow and hand component. Since the kinematic synergy does not apply between the shoulder and hand, when the hand control is active, the prosthesis utilizes the standard proportional EMG control (i.e., equation (2)). When the elbow control is active, the prosthesis utilizes the coordinated control equation (i.e., equation (4)). Rather than use co-contraction to switch between the two controllers, the coordinated controller is further modified (relative to the standard sequential control) to leverage the presence of the IMU to facilitate the process of switching between hand and elbow control. Specifically, when the elbow velocity (4) remains essentially zero for a short duration, and when both components on the right-hand side of (4) also remain essentially zero for this duration (i.e., both the upper arm angular velocity and EMG command are zero), the prosthesis control is automatically switched to the hand. Note that this condition implies that the hand is essentially remaining fixed relative to the user's body, such as would be the case if a user were about to grasp a stationary object. When in the hand control state, as previously mentioned, the hand is controlled by (2). When in this state, and when the upper arm angular velocity becomes essentially non-zero (i.e., the upper arm begins to move in the plane orthogonal to elbow rotation), the EMG control automatically switches back to the elbow. In this manner, all elbow movement must by initiated by shoulder movement. The use of this rubric obviates the need to use co-contraction to toggle control between components. As such, co-contraction can either be eliminated from the control structure, or can be preserved for use for the control of other components. Fig. 6 shows a FSM of the coordinated controller, depicting the switching structure of the coordinated control approach.

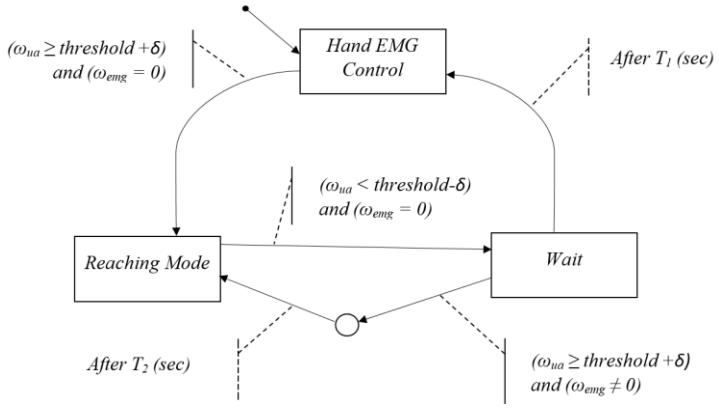

Fig. 6. FSM of coordinated elbow/hand control structure

4.3.3 Experimental implementation and assessment

The relative performance of the coordinated controller was assessed and compared with a conventional sequential EMG control approach in a set of experiments in which six healthy subjects performed several different pick-and-place tasks within a virtual environment. The virtual tasks were performed with a virtual transhumeral myoelectric prosthesis, which was alternately controlled using either the standard sequential EMG controller or the previously described coordinated controller. The virtual environment enabled both a well-controlled experimental environment, and a well-controlled assessment of performance.

A. Virtual Assessment Task

The virtual assessments consisted of a series of pick-and-place tasks in which each subject was required to pick up a ball resting on a table and place the ball into a target box, which was randomly positioned in one of twelve target locations. The twelve target locations corresponded to a spatial matrix of box locations, configured to be two boxes across, three boxes high, and two boxes deep. Each box (i.e., cell) was open in the front and approximately cubic, with a characteristic dimension approximately twice the ball diameter. See representative cell in Fig. 7.

A trial consisted of 36 pick-and-place tasks, in which each targeted location appeared three times in a randomized order. A representative pick-and-place task is depicted in the sequence of screen shots shown in Fig. 7, where the activity associated with each frame is described in the caption. The details of the virtual environment in which the tasks were performed are given in the following subsection.

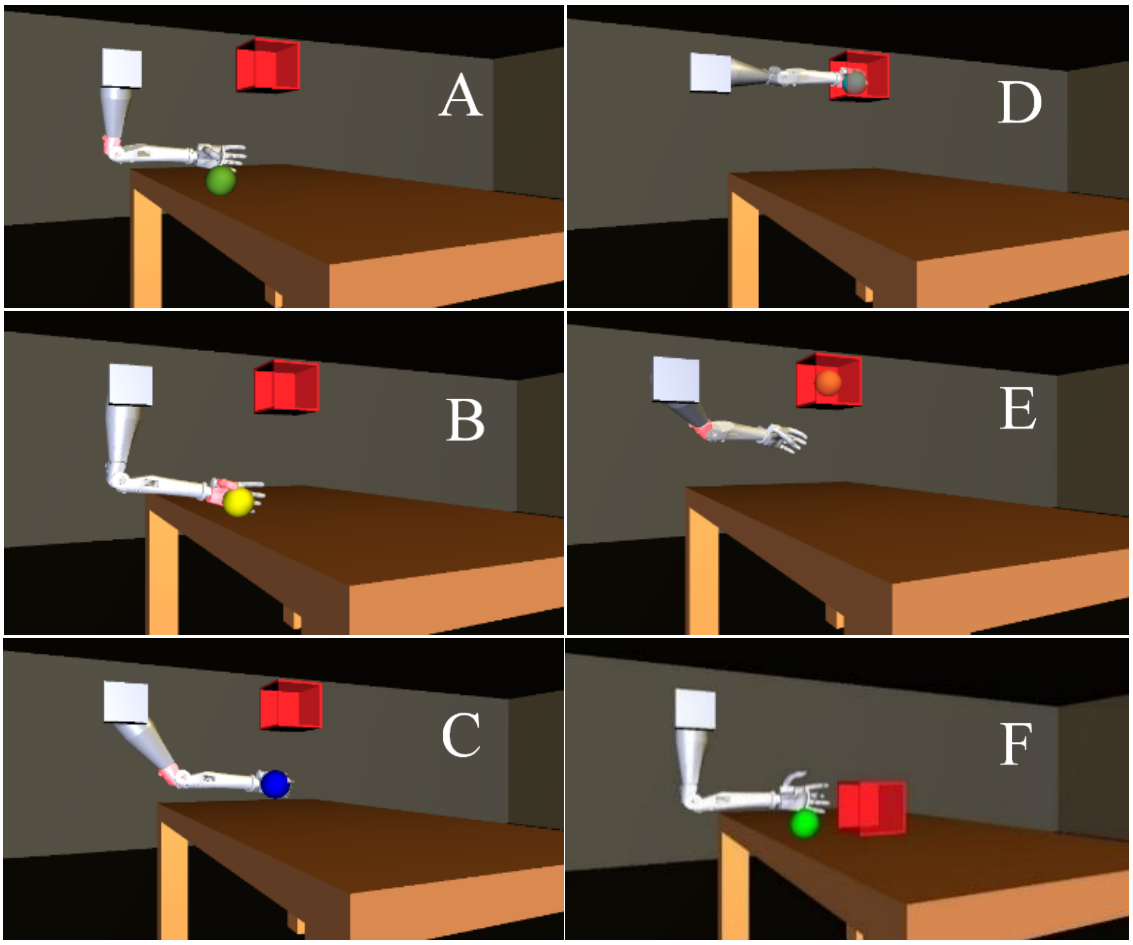

Fig. 7. The virtual environment used in the controller assessments. (A) The elbow joint starts each task fully extended, and must be controlled by the user to configure the arm to pick the ball. (B) The hand starts fully opened; the ball changes color from green to yellow when the hand is positioned to grasp it; the hand must be closed by the user around the ball in order to grasp it; the ball changes color from yellow to blue to indicate that it has been grasped. (C) Once grasped, control is switched to the elbow to perform the reaching motion toward the target box. (D) The ball must be positioned in the middle of the box, after which it changes color to light blue, to indicate that it is ready to be released. Control must be switched to the hand to release the ball. (E) After successful release, the ball changes color to orange, the completion time is recorded, and (F) a new ball and box appear for the next reaching task. The tasks are performed continuously, such that the timer for the next task starts when the ball is released from the previous task.

B. Virtual Environment

The virtual environment in which the assessments were performed included an 8-DOF virtual arm, where the 8-DOFs included: 1) the three-dimensional location of the shoulder joint within the virtual space (3 DOFs); 2) the angular orientation of the upper arm in the virtual space (3 DOFs); 3) the elbow angle (1 DOF); and 4), the hand configuration, which in this case was a single-DOF device, the grasp of which was characterized by a single angle and corresponding angular velocity (1 DOF). As described subsequently, instrumentation on each subject provided real-time input that defined motion of the upper arm and shoulder DOFs, such that the upper arm and shoulder tracked in real-time the physical motion of each subject. Motion of the elbow and hand DOFs, however, were based on the (real-time) output of either the sequential or coordinated arm controllers, depending on which controller was being used at any given time. These controllers were driven by real-time EMG measurements from the user's healthy arm, and in the case of the coordinated controller, an IMU affixed to the subject's arm to measure upper arm angular velocity. Thus, the virtual arm emulated a transhumeral prosthesis, in which the torso and upper arm movement tracked in real-time the corresponding movement of the seated subject, while both the hand and elbow components of the prosthesis were controlled via real-time EMG measured from the subject (in the case of the sequential controller), or by both real-time EMG and IMU measurement (in the case of the coordinated controller).

In addition to the arm, the virtual environment also included a table, a small ball (approximately the size of a baseball or tennis ball) that can be grasped, held, and released by the hand, and a small box, in which the ball can be deposited. The box was alternately located in one of twelve target locations, in order to cover a representative workspace of reaching motions.

4.3.4 INSTRUMENTATION AND APPARATUS

In order to perform the assessments, each subject was instrumented with sensors to provide real-time input to drive the virtual prosthesis. Measurement of torso motion was also used to characterize movement of the torso for purposes of performance assessment. In total, the experimental instrumentation consisted of: 1) a pair of EMG electrodes; 2) an elbow immobilizer; 3) an upper arm-mounted IMU; and 4) a trunk-mounted IMU. The trunk IMU was not used for prosthesis controller input, but rather was used to 1) provide Cartesian motion of the trunk (i.e., shoulder joint) relative to the task frame to drive the virtual torso motion and 2) to characterize compensatory movement of the trunk. The upper arm IMU was used to provide upper arm motion in the task frame, in order to drive the movement of the virtual upper arm, and also as an input to control the prosthesis for the coordinated control approach. Since movement of the intact elbow, wrist, and hand were not used in the experiments, a hand, wrist, and elbow joint immobilizer was employed to preclude movement of the (non-virtual) joints during the experiments and better represent the muscular conditions in the residual limb of an amputee subject. Use of the immobilizer, however, impinged on the upper arm EMG electrodes and obstructed upper arm EMG measurement. In order to provide unobstructed EMG input for the prosthesis controller(s), the EMG electrodes were moved to the forearm, where they were free of impingement by the immobilizer. Although such placement is less representative of the musculature employed by transhumeral amputees, since both controllers employed the same EMG sites in the same manner (i.e., equation (2)), any substantial effect from this modification should wash out of the comparison, thus indicating the relative value of superimposing the synergistic component of control on top of the EMG component.

A. EMG Measurement and Signal Conditioning

EMG data was acquired using two disposable conductive gel Ag/AgCl electrodes (Norotrode 20, Myotronics, Inc.) positioned over the subject's anterior and posterior surfaces of the left forearm with a reference electrode positioned proximal to the elbow. The acquired raw EMG signals of the electrodes were preamplified with a gain of 100 and digitally sampled using an EMG processing chip (Texas Instruments ADS1298), which also provided bandpass filtering (between 20 Hz and 500 Hz) and rectification. The rectified signal was sent via serial peripheral interface (SPI) to a PIC32 microcontroller (Microchip, Inc.), where it was low-pass-filtered at 5 Hz to provide an envelope of spatially integrated EMG activity. The (two) processed EMG signals were then streamed from the PIC32 via a controller area network (CAN) bus to the real-time environment provided by Simulink Real-Time Workshop (RTW)

B. Shoulder/Arm Angular Velocity Measurement

An IMU was incorporated on the same circuit board used for EMG data acquisition and signal processing, which was affixed to the arm immobilizer affixed to the subject's upper arm. The IMU used for upper arm motion was a high-performance 9-axis unit that combined a 3-axis accelerometer, 3-axis gyro, and 3-axis magnetometer that provided high-bandwidth real-time three-dimensional orientation of the upper arm (VectorNav Technologies VN-100 SMD). The upper arm orientation measurement was sent from the IMU to the PIC32 via an SPI bus on the board, and then streamed from the PIC32 to the RTW environment via a CAN bus. This measurement was used to both drive the upper arm orientation within the virtual environment (for both controllers), and also to provide the angular velocity command for the coordinated controller.

C. Torso Motion Measurement

The torso motion was measured using a separate 6-axis IMU (Invensense MPU-6555) mounted to a separate circuit board via an elastic band to the center of each subject's chest, approximately at the xiphoid process. The torso IMU sent 3-axis acceleration and 3-axis gyroscopic information to a PIC32 via an SPI bus, which streamed the data via a CAN bus to the RTW environment. The acceleration and angular velocity signals were combined with the RTW environment with a complementary filter using a crossover frequency (between the accelerometer and gyroscope) of 1 Hz (i.e., the roll-off for both the low-pass and high-pass filters of the fused data), which provided real-time torso orientation in both the sagittal and coronal planes, which was in turn used to: 1) drive the torso motion within the virtual environment, and 2) provide a measure of compensatory motion during the experiments. Note that the experiments assume that the subject's chair remains stationary during the experiments (which was consistent with the conduct of the experiments).

4.3.5 HUMAN SUBJECTS

Six healthy, non-amputee subjects participated in the experiments, which were approved by the Vanderbilt University Institutional Review Board. Each subject participated in five trials for each controller where, as stated above, each trial consisted of 36 pick-and-place tasks. All subjects were seated in a chair in front of the computer monitor, which remained in a fixed location once the trial began. Subjects were required to use their left arm in the experiments, since both the instrumentation and virtual prosthesis model were configured for the left arm. The trials for each subject were generally conducted over a one-week period. In order to account for order effects, half of the subjects used the sequential controller first, followed by the coordinated controller,

while the other half of subjects performed the trials in the reverse order. Note that each subject was required to complete each pick-and-place task – if the ball was dropped prior to placement in the box, the ball would be automatically reset in the starting position for the subject to re-attempt the task, until the task was successfully completed. Once the task was successfully completed, the ball was reset in the starting position, and another target location (i.e., box location) was randomly presented.

4.3.6 SUBJECT TRAINING

For each subject, an initial session was used to establish EMG thresholds and normalization gains, followed by an introduction to the control method, and a practice period during which the subject could practice controlling the elbow and hand, and could practice performance of the pick-and-place tasks. The duration of the training/practice phase varied by subject, but typically lasted between 15 and 30 minutes, as per each subject's preference. Once sufficiently practiced, the subject performed a series of trials with the prescribed control approach, each consisting of 36 pick-and-place tasks. The completion times associated with each of the pick-and-place tasks were recorded, in addition to the torso motion during the respective trials. Once each subject had completed the series of five trials using the assigned controller, the subject was introduced to the other control approach, and aside from calibration of the EMG, followed the same process of training and evaluation.

4.3.7 CONTROLLER THRESHOLDS AND GAINS

The two elbow controllers collectively employ four controller gains, which were established for each subject prior to performing the virtual assessments. Note that once these gains were established, they were maintained in the controller for each subject throughout all experimental

sessions (i.e., for the several-day duration of the each subject's involvement in these experiments). The gains k_1 and k_2 ensure that the maximum EMG for each subject and each EMG channel corresponds to a maximum elbow angular velocity. These were established in pre-trial experiments for each subject, in which several maximum voluntary contractions were performed, and the respective gains were established by correlating the mean EMG corresponding to the contraction with the maximum commanded elbow angular velocity (set at 50 deg/s). The coordinated controller also employs two additional gains, k_3 (which determines the degree of kinematic coupling between the shoulder and elbow) and k_4 (which determines the relative weighting of EMG command to IMU command in the controller. For all trials and all subjects, both these gains were set to one. As such, in the absence of EMG, elbow extension angular velocity would exactly equal shoulder flexion angular velocity, while in the absence of shoulder motion, the coordinated controller reduced to exactly the sequential EMG controller.

4.4 RESULTS

4.4.1 REPRESENTATIVE ELBOW CONTROLLER RESULTS

Fig. 8 through Fig. 11 show controller data during performance of a representative pick-and-place task (i.e., while picking and placing the ball into box number 2) while using the sequential EMG controller and the coordinated controller, respectively.

Fig. 8 shows the EMG command over the task performance period, where the gray bands indicate periods of hand control and the white bands indicate periods of elbow control. One can note the co-contraction "spikes" in the EMG signals that separate the period of hand and elbow control. The essential features of the EMG correspond to: 1) co-contraction to switch to elbow control; 2) flexing the elbow to position the hand at the ball (~0-4 s); 3) co-contraction to switch

to hand control; 4) grasping the ball (~4-8.5 s); 5) co-contraction to switch to elbow control; 6) extending the elbow (while flexing the shoulder) to reach out toward the box (~8.5-14 s); 7) co-contraction to switch to hand control; and 8) releasing the ball (~14-16 s). The asterisk at the end of the data indicates task completion (in this case at ~16 s). Fig.9 shows for the same representative pick-and-place task the EMG angular velocity command (equation 1) during periods of elbow control only, showing the initial period of elbow flexion and subsequent period of elbow extension, and also shows the root-mean-square (RMS) value of elbow angular velocity command over the duration of the task, which has a value of 22.8 deg/s (i.e., the elbow joint moved with an average angular velocity of 22.8 deg/s during the task).

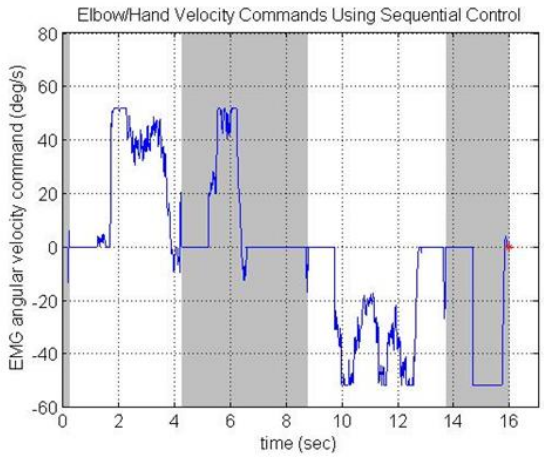

Fig. 8. Arm (elbow and hand) velocity commands during a representative pick-and-place task (box no. 3) performed with the sequential EMG controller. The gray bands indicate the periods of hand control, while the white bands indicate the periods of elbow control.

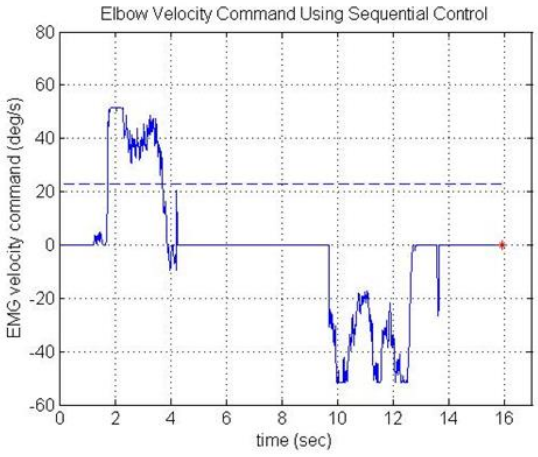

Fig.9. Elbow velocity commands during a representative pick-and-place task (box no. 3) performed with the sequential EMG controller, and RMS average of elbow EMG angular velocity command over the task duration (dashed line).

Fig. 10 shows the corresponding controller data, for the same subject, during the same pick-and-place task (i.e., box number 3), while using the coordinated controller (i.e., equation 3),

showing both the IMU component of elbow angular velocity (equation 2) and the EMG component (equation 1), over the entire task performance period. Since the weighting gains are unity, the total elbow angular velocity command (equation 3) is the direct sum of these components. As in Fig. 8 the gray bands indicate periods of hand control and the white bands indicate periods of elbow control. As in Fig. 8 the periods of activity correspond to positioning the elbow to pick up the ball, grasping the ball, extending the elbow (and flexing the shoulder) to place the ball, and releasing the ball. The asterisk at the end of the data indicates task completion (in this case at ~10.5 s). Note that co-contraction is not present at the transitions between elbow and hand control, since it is not used in the coordinated controller. Fig. 11 shows for the same data the IMU and EMG angular velocity commands during periods of elbow control only, and also shows the root-mean-square (RMS) values of the respective commands. For this task, the average RMS angular velocity command resulting from the IMU component was 16.0 deg/s, while the RMS command resulting from the EMG component was 12.0 deg/s. As such, for this representative task, the majority (~60%) of elbow movement resulted from the IMU component. Further, the average speed of elbow movement across the trial was 28.0 deg/s (the sum of the components), which is approximately 27% faster than the corresponding average speed with the sequential control approach.

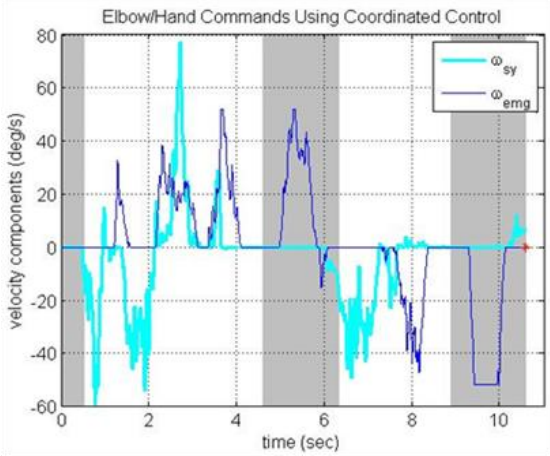

Fig. 10. Arm (elbow and hand) velocity commands during a representative pick-and-place task (box no. 3) performed with the coordinated controller, showing both the EMG and the IMU components of angular velocity command. The gray bands indicate the periods of hand control, while the white bands indicate the periods of elbow control

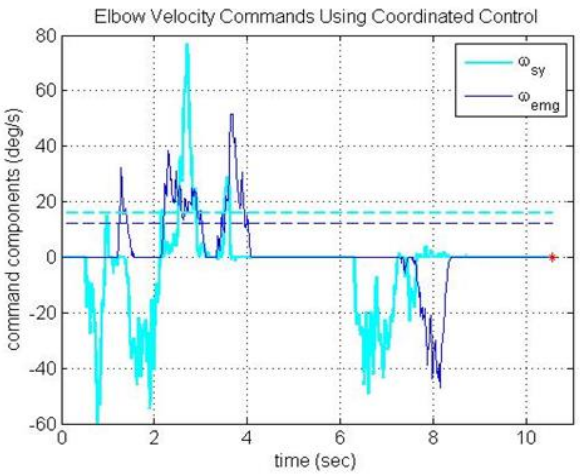

Fig. 11. EMG (thin dark trace) and IMU (thick light trace) elbow angular velocity commands during a representative pick-and-place task (box no. 3) performed with the coordinated controller, and corresponding RMS averages over the task duration (dashed lines).

4.4.2 VIRTUAL TASK PERFORMANCE RESULTS

Fig. 12 shows the distribution of task completion times averaged across all subjects for each of the five trials, for each controller type. Fig. 12 also shows the mean completion time for each trial across all subjects, which is the black line connecting all trials. Note that all subjects demonstrated a general learning trend consistent with the mean. The numerical values of the mean completion times corresponding to each trial, in addition to the standard deviation for each, are enumerated in Table IV.

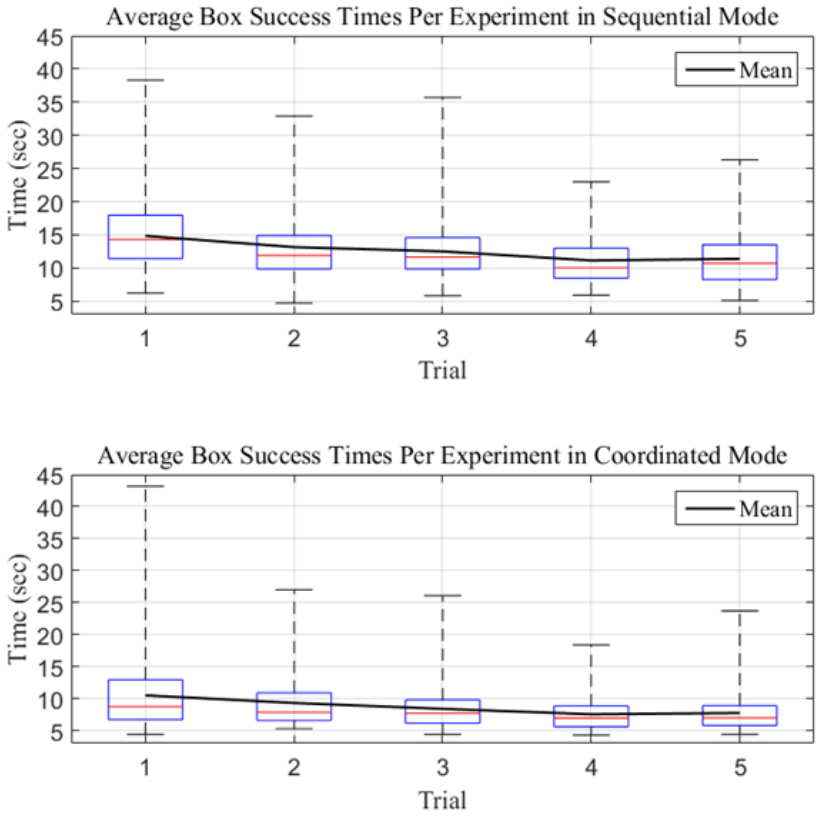

Fig. 12 Distribution of task completion times averaged across all subjects for each of the five trials, for each controller type

Table IV

AVERAGE TASK COMPLETION TIMES

Trial	Sequential Completion Times (s)	Coordinated Completion Times (s)
	mean (SD)	mean (SD)
1	14.8 (5.0)	10.5 (5.5)
2	13.1 (4.9)	9.3 (4.0)
3	12.5 (3.9)	8.4 (3.1)
4	11.1 (3.8)	7.6 (2.5)
5	11.4 (3.9)	7.8 (2.7)
Average trials 3-5	11.7 (3.9)	7.9 (2.8)

In order to account for learning, performance data was only considered after the average performance reached essentially a steady-state condition, which was defined by the authors as the case when the mean completion time varied by less than 10% between trials. Based on this criterion, the last three trials were considered for the performance assessment. Specifically, for the sequential controller, the mean completion time for the last three trials fall within 7%, 5%, and 2% of the 3-trial mean, respectively. For the coordinated controller, the last three fall within 6%, 4%, and 2%, respectively, of the 3-trial mean. As such, trials 3 through 5 only were considered for the performance assessment. As given in Table IV, the average task completion time for the sequential controller (across all subjects and across trials 3 through 5) was 11.7 s, while the average task completion time for the coordinated controller (also across all subjects and trials 3 through 5) was 7.9 s. As such, the coordinated controller enabled completion of the pick-and-place tasks on average 32% faster than the sequential controller (i.e., the tasks were completed with the coordinated controller in 68% of the time required by the sequential controller). The average task completion times for each target box location, averaged across the last three trials and across all subjects are shown in Fig. 13. As shown in the figure, the task completion times were reduced consistently across all pick-and-place tasks (i.e., across all target box locations). As such, the proposed method appears to provide a consistent performance advantage, relative to the sequential approach, for all reaching movements represented in this study (i.e., the method appears to provide a performance advantage regardless of specific reaching location). A paired t-test was performed for the distribution of completion time data corresponding to each of the locations, indicating that the difference in means in all cases was significant with greater than a 99% confidence level.

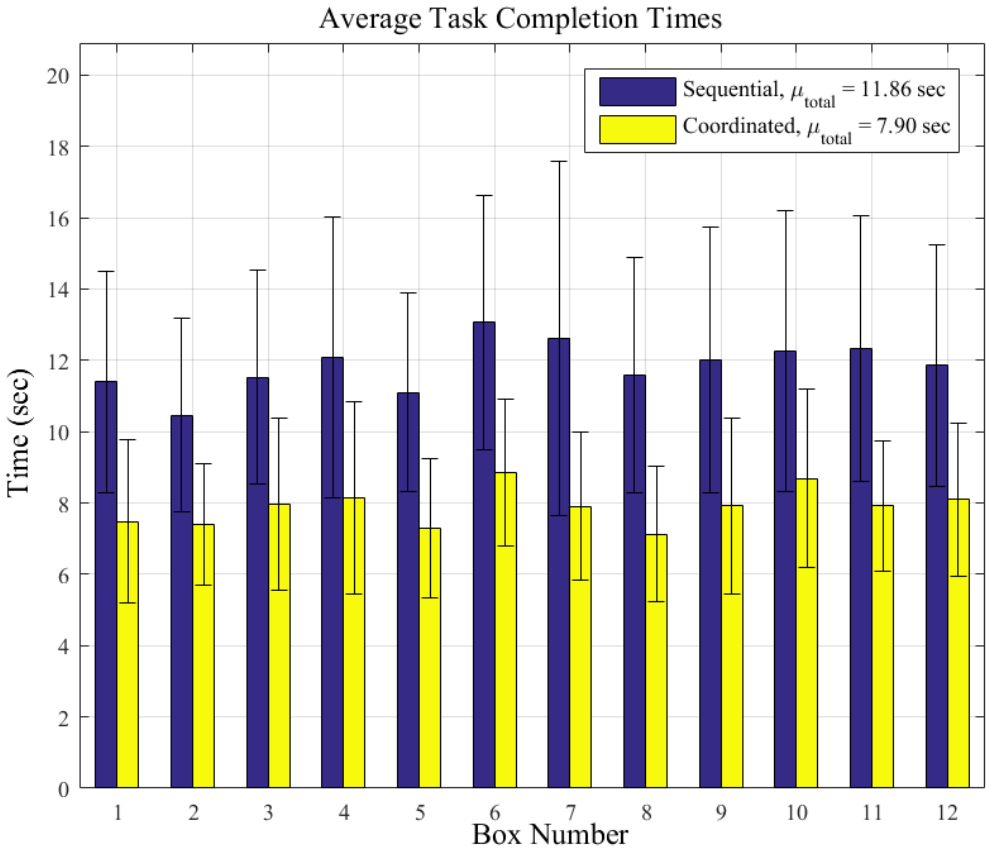

Fig. 13 Average task completion times across all subjects and trials, corresponding to each respective target box location, representing a variety of reaching movements.

In addition to task completion time, each subject's performance of each task was also characterized by the compensatory torso motion employed for each pick-and-place task. Specifically, the torso angles, with respect to the vertical, in the sagittal and coronal (or frontal) planes were recorded at the time each reaching task was completed (i.e., when the ball was successfully released in the target box). These measurements in effect characterized the torso configuration upon completion of each reaching task, and specifically how much forward and sideways lean was employed to reach the target location. The magnitude of respective torso angles, averaged across all subjects for each target location and each controller type, are shown in Fig. 14, and Fig. 15, respectively, along with error bars indicating plus and minus one standard deviation

for each. Although slight differences exist in the means, a paired t-test of the data indicates in all cases that the average compensatory torso motions are not statistically different between the two controllers, for all target locations and for both biomechanical planes of movement. As such, task completion times were on average 37% faster with the coordinated controller, with no difference in compensatory torso motion.

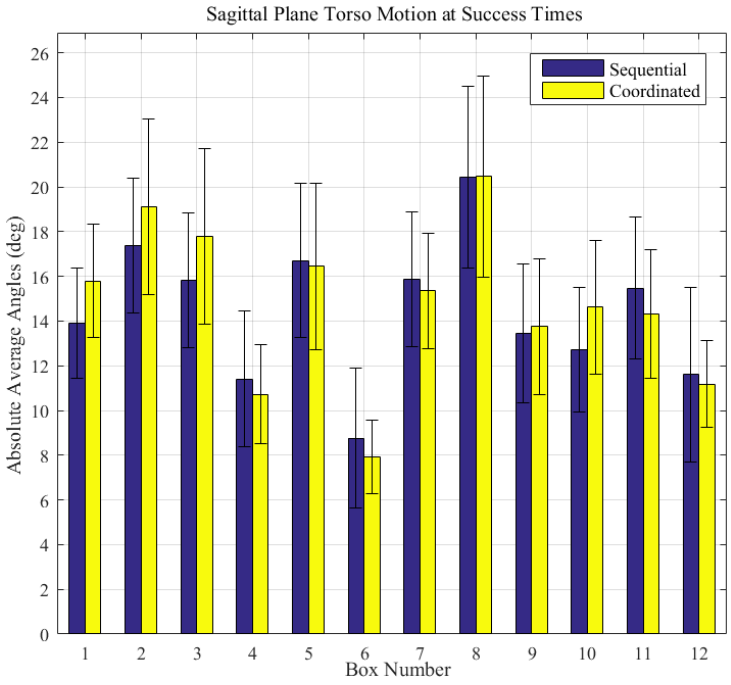

Fig. 14 Comparison of the average forward lean employed to reach each target location.

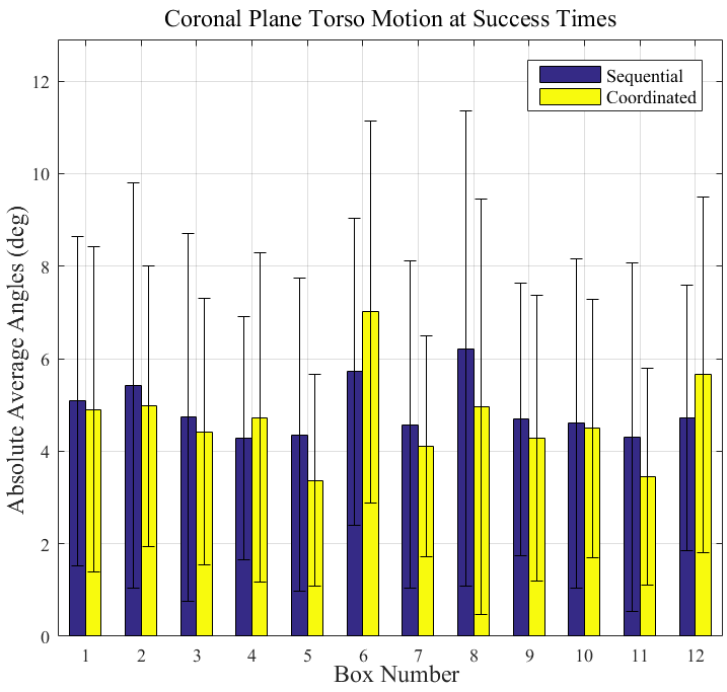

Fig. 15 Comparison of the average sideways lean employed to reach each target location.

4.4.3 SUBJECTIVE FEEDBACK

Although subjective feedback has clear limitations, following the trials, subjects indicated that the synergistic method of elbow control provided more intuitive elbow movement that was easier to use than the EMG-only (sequential) elbow controller. Subjects also reported that switching between hand and elbow control was considerably easier without the need for co-contraction.

4.4.4 LIMITATIONS

Based on the virtual experiments, use of an EMG-modulated shoulder/elbow synergy, combined with an IMU-based approach to toggling between active components, appears to provide a significant reduction in task completion times for pick-and-place reaching tasks, without altering

the extent of corresponding torso motion. Limitations in the study include: 1) use of healthy rather than amputee subjects; 2) use of a virtual rather a physical environment; 3) use of a virtual rather than physical prosthesis; 4) use of forearm rather than upper arm EMG; and 5) only reaching tasks were characterized. Another limitation of this study is that the data does not explicitly indicate the relative functional value provided by the IMU component of the elbow controller, versus the value of using the IMU to perform switching of control between the hand and elbow components. Finally, the authors note that, while a myoelectric wrist was not employed in this study, the control method could be used with one. Since EMG co-contraction is not required for switching between control of the elbow and hand with the proposed approach, such co-contraction can be reserved for switching between control of a myoelectric hand and wrist (i.e., there is one less component associated with EMG multiplexing). Alternatively, although beyond the scope of this paper, methods similar to that proposed could be developed by extracting control information from the IMU and fusing it with EMG in order to facilitate improvements in the control of a myoelectric wrist joint.

4.5 CONCLUSION

This paper proposed a control method for the control of a transhumeral prosthesis with myoelectric hand and elbow components. The control method supplements the standard two-site EMG control with an IMU, which provides 1) coordinated motion between the (prosthetic) elbow and (intact) shoulder joints, and 2) automatic switching between hand and elbow control (i.e., based also on movement of the intact shoulder). The authors conducted an assessment of the coordinated control approach on six healthy subjects in a virtual environment involving a series of pick-and-place tasks, where location of the object placement were varied widely. Results from this assessment indicated that subjects were on average able to complete the tasks 32% faster with the

coordinated controller, relative to completion with a traditional sequential transhumeral myoelectric control approach, without affecting the extent of compensatory torso movement. In future work, the authors plan to conduct these assessments with amputee subjects using a myoelectric transhumeral prosthesis.

4.6 ADDENDUM

The coordinated controller design went through several iterative stages before converging to its final version which was described in the above manuscript. The work presented in the manuscript involved building Simulink models, designing the electronics board, writing the code for the embedded systems in C language, and building the virtual environment in order to build an effective test-bed to investigate different control methodologies for transhumeral prostheses. As described in the manuscript, the coordinated controller leverages movement synergies between the intact shoulder joint and prosthetic elbow joint, particularly during reaching movements. Several versions of coordinated controller were investigated during the development. The following sections illustrate some of the implemented versions of the controller.

4.6.1 COORDINATED CONTROLLER VERSION I

The first version of the coordinated controller attempted to coordinate the motion of the elbow and intact shoulder joint with the ability to control the hand and elbow simultaneously. Fig. 16 illustrates the state chart of the first version of the coordinated controller. In this version, the user controlled the hand via the EMG signal as in (2), and if a co-contraction was detected, the controller switched to elbow EMG control mode, similar to a traditional sequential controller where both hand and elbow are controlled as given in (2). However, if the upper arm angular velocity (ω_{ua}) was greater than a certain threshold, the controller switched to a coordinated control

state where the elbow position was a function of the upper arm angular velocity (ω_{ua}) and the elbow control given by:

$$\omega_{eb} = \omega_{sy} \tag{5}$$

Also, in this state, the EMG signal controlled the hand (as given in (2)) which allowed the simultaneous control of the elbow (using the upper arm angular velocity as given (5)) and hand (using the EMG as given (2)). While in the coordinated control state, if the upper arm angular velocity (shoulder angular velocity) dropped below a certain threshold, the controller switched to the sequential control state where the user could adjust the position of the elbow using EMG signal or co-contractions to switch the control mode to hand EMG control.

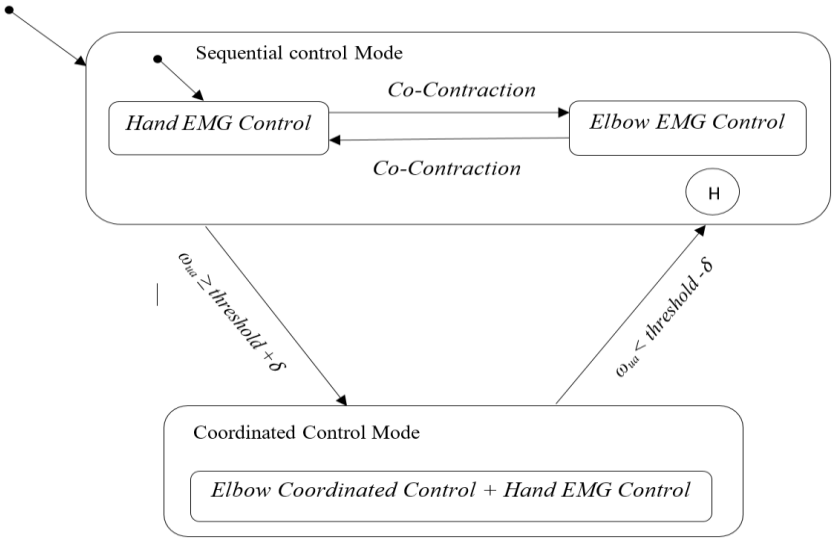

Fig. 16. First Version of Coordinated Controller Finite State Machine

Even though this version of the coordinated controller coordinates the elbow position with the intact shoulder motion and allows simultaneous control of both hand and elbow, the co-contraction signal still needed to switch the EMG signal to hand control if EMG signal is controlling the elbow.

Also, adjusting the elbow angle requires ω_{ua} to drop below a certain threshold. Observations of the experiments using this controller indicated that it relied heavily on the co-contraction signal. The performance of the controller in performing reaching task was degraded using this controller due to frequent switching using co-contraction and inability to modulate the elbow angle during the reaching task. In addition, co-contraction was physically tiresome during reaching tasks. Furthermore, simultaneous hand/elbow control is not needed in simple reaching tasks and adjusting the elbow position requires changing the arm configuration (i.e., $\omega_{ua} <$ threshold $- \delta$ or $\omega_{ua} \geq$ threshold $+\delta$).

4.6.2 COORDINATED CONTROLLER VERSION II

The second version of the coordinated controller utilized co-contraction in both of the states of the controller in order to better utilize the switching signal as presented in Fig. 17. In other words, when the controller was in the coordinated control mode, if a co-contraction was detected, the controller switched to a locked state where the elbow position was locked and EMG controlled the hand as in (2). This version maintained the same sequential control mode state and transition conditions as in the first version. The main difference in this version is the addition of the elbow lock state, which the controller transitioned to when in the coordinated control state and a co-contraction signal was detected.

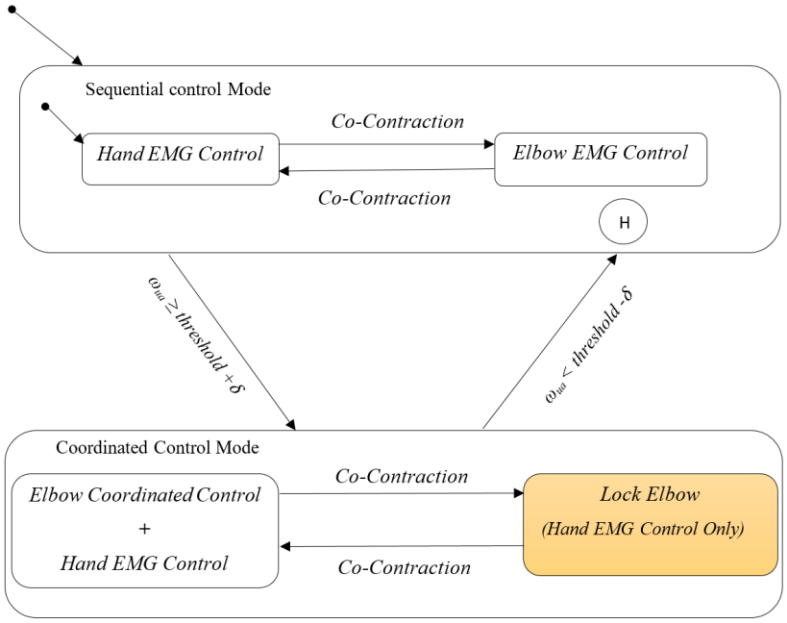

Fig. 17. Second Version of Coordinated Controller Finite State Machine

By having a locked state, the user was able to move the arm in space while maintaining the elbow position with the ability to control the hand using EMG. With the further testing, locking the elbow position is an important feature in reaching tasks that the first version didn't have; however, co-contraction was still required as a switch signal to switch to either the hand or elbow when the controller was in the coordinated control state. Therefore, the same drawbacks of the first version persist in this version.

4.6.3 COORDINATED CONTROLLER VERSION III

The previous versions of the coordinated controller used co-contraction to switch between hand control and elbow control or to lock elbow position. The experimental results of the previous versions showed a slow performance during reaching tasks due to use of co-contraction to frequently switch between the two controls components (hand/elbow). Therefore, the third version of the coordinated controller relied heavily on the IMU to minimize the use of co-contraction.

Specifically, in the sequential control mode, co-contraction was still used to switch between the hand and elbow control and both components (hand or elbow) were controlled as given in (2); however, the transition to coordinated control mode was performed by moving the intact shoulder joint in the coronal plane. Such movement in the coronal plane allows the gyroscope to detect the angular velocity of the subject's upper arm in the corresponding plane ($\omega_{ua\text{-}y}$). If the $\omega_{ua\text{-}y}$ exceeds a certain threshold, the controller switches to the coordinated control mode. Fig. 18 illustrates the FSM of the version of the coordinated controller.

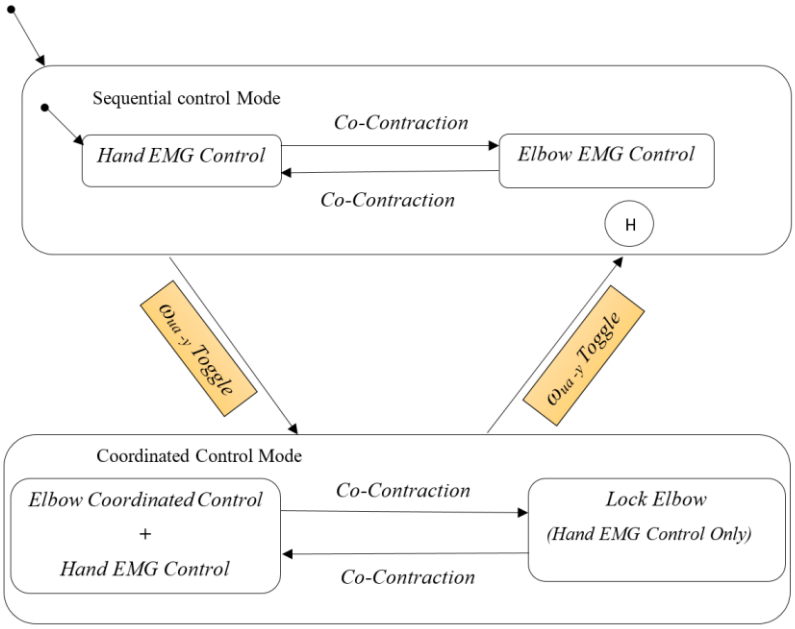

Fig. 18. Third Version of Coordinated Controller Finite State Machine

The two states (sequential control mode and coordinated control mode) of the previous versions of the coordinated controller were still used in this version, however, the transition between the two states was performed by a flick motion instead of a co-contraction. The flick motion enhanced the temporal performance of the coordinated controller but degraded the spatial performance. For example, the user manipulated the arm to position the hand in order to pick an

object, once the object is picked up, then the user needed to flick to switch to a coordinated control mode where the elbow position was controlled by the upper arm angular velocity and the superimposed EMG command as in (4). Once the hand was in the target position and the user needed to adjust the elbow position, the user flicked again to adjust the elbow position using EMG, which causes the hand to deviate from the target location and the user needed to re-configure the arm to position the hand in the target location and then the user needed to either flick or co-contract to open the hand to place the object. In this version of the controller, the user needed to remember the last state before the transition occurred, which increased the cognitive load and reduced the level of intuitiveness using the controller. In addition, more training was needed to learn the use of the controller.

4.7 SUMMARY

Observations from the previous versions indicated that, neither the co-contraction signal nor the flick motion seem to enhance the level of intuitiveness using the coordinated controller. The co-contraction slowed the performance of the coordinated controller during reaching tasks. The flick signal is an interesting switch signal; however, reconfiguring the arm after every flick signal is required for accurate positioning of the hand, which also slowed the performance during reaching tasks. These drawback were taken into consideration in the final version of the coordinated controller which is described in the manuscript. Following the experiment presented in the manuscript, subjects indicated that the coordinated controller provided more intuitive elbow movement that was easier to use than the EMG-only (sequential) elbow controller. Subjects also reported that switching between hand and elbow control was considerably easier without the need for co-contraction.

CHAPTER 5

ASSESSING A COMBINED IMU/EMG CONTROL APPROACH IN A MYOELECTRIC TRANSHUMERAL PROSTHESIS

5.1 ABSTRACT

This paper describes the implementation and assessment of an IMU-enhanced controller for a transhumeral myoelectric prosthesis. The controller supplements EMG commands with information from a prosthesis-mounted IMU, with the objective of improving the efficacy of control of a myoelectric hand/elbow prosthesis. The controller was implemented on a myoelectric transhumeral prosthesis prototype, and tested on a single transhumeral amputee subject in a series of pick-and-place tasks, in which the subject used the combined IMU/EMG controller, and also a conventional EMG-only controller. Results of these assessments indicate that subject was able to perform the pick-and-place tasks approximately twice as fast on average with the combined IMU/EMG control method, relative to the conventional EMG method.

5.2 INTRODUCTION

Surveys of upper limb amputees indicate a general desire for improved function in their prostheses [18, 27, 59, 60]. Among the preferences for users of transhumeral prostheses in particular is the desire to "coordinate motions of two joints at the same time" [27]. Transhumeral prostheses are typically controlled by the electromyogram (EMG) from an agonist-antagonist muscle pair (specifically the EMG from the biceps and triceps brachii muscle groups), which together provide a single bi-directional control signal. Since a myoelectric transhumeral prosthesis typically includes at least a myoelectric hand and elbow, the single EMG control channel must be

switched (or multiplexed) between control of the hand and elbow component, such that movement of each component is conducted in a conventional EMG manner. In a typical prosthesis, switching the EMG control between arm components (i.e., between the hand and elbow) is conducted via brief co-contraction of the agonist-antagonist muscle pair. Conventional EMG controlling the arm components is simple and robust, but considerably less efficient than the simultaneous joint movement observed during healthy arm function. Various approaches have been developed to improve the efficacy of EMG-controlled myoelectric transhumeral prostheses, including the use of pattern recognition techniques (see, for example, [61-63]), neural network approaches [64], and predictive control techniques [65].

Rather than use EMG as the sole communication and control channel between the user and prosthesis, this paper employs a controller that supplements EMG with information from an inertial measurement unit (IMU) mounted on the prosthesis. The IMU specifically provides information about the movement of the residual limb (i.e., upper arm motion), which therefore provides additional information about movement intent. The use of IMUs to supplement the control of lower limb prostheses has been well-documented [66], and researchers have recently begun to exploit them to improve control of upper limb prostheses [57, 58, 67, 68]. Unlike EMG information, an IMU can provide information about movement of the residual limb in space that is not encoded in, or difficult to extract from EMG alone, and thus an IMU adds information regarding the volition, movement, and potentially the movement intent of the user. In previous works, the authors have proposed a control approach that supplements a standard two-channel transhumeral EMG interface (i.e., biceps and triceps) with information from a prosthesis-mounted IMU. The control method consists primarily of two components. First, the IMU is used to provide a nominal elbow joint movement that is coupled to the upper arm movement (as measured by the

IMU), such that shoulder joint flexion results in elbow joint extension. The EMG is then used as it typically would be in an EMG-controlled elbow, but the movement commanded by the EMG is superimposed onto the nominal shoulder/elbow coupling. Second, rather than require a brief co-contraction to switch the EMG between the elbow and hand components, the controller uses the IMU to detect whether or not the hand is moving in space, and automatically switches control to the hand when it is still, and to the elbow when the hand is moving. In a prior paper, this control approach was assessed in a set of experiments on healthy subjects in a virtual environment, and shown to provide improved ability to conduct pick-and-place tasks relative to a conventional EMG control approach as described in the previous chapter. In this paper, the authors have implemented the control approach in a myoelectric transhumeral prosthesis prototype, and conducted an assessment of the control approach on a single subject, comparing the ability of the subject to perform pick-and-place tasks with the combined IMU/EMG control approach, relative to her ability to perform the same tasks with a conventional EMG control approach.

5.3 CONTROL METHODS

This section briefly describes the conventional control method, referred to as conventional EMG control, and the proposed control approach, referred to as combined IMU/EMG control. Both the conventional EMG and combined IMU/EMG control approaches utilize a standard two-site EMG electrode interface, corresponding to one electrode over the biceps muscle group, and one over the triceps in addition to a reference electrode. These controllers are described in the previous chapter, and therefore only summarized here. Note that both controllers incorporate identical (and standard) signal conditioning of the EMG measurements, which includes a bandpass filter stage (to remove DC potentials and high-frequency noise), followed by a rectification and

additional low-pass filter stage (to provide the magnitude envelope of spatially integrated EMG activity).

5.3.1 CONVENTIONAL EMG CONTROL

In the conventional EMG control mode, control of either the elbow or hand is selected at any given time by a short-duration co-contraction of both EMG inputs, which toggles the control to one of the two components. The component not being controlled assumes a locked state. When a component is under EMG control, the differential measurement of the two-site EMG is used to generate a velocity command, such that the user contracts the residual limb musculature to induce movement, and relaxes limb musculature to maintain the current configuration. Thus, if e_1 and e_2 represent the filtered and rectified EMG from the biceps and triceps muscles, respectively, the angular velocity command for the active component is given by (2).

Typical signal conditioning such as hysteresis and a dead band around an EMG noise floor are incorporated to facilitate well-behaved, deliberate control. As previously mentioned, the EMG control (2) is switched between the hand and elbow components using a brief co-contraction of the two EMG signals (e_1 and e_2). The finite state control structure that governs the switching between the hand and elbow components is shown in Fig. 19.

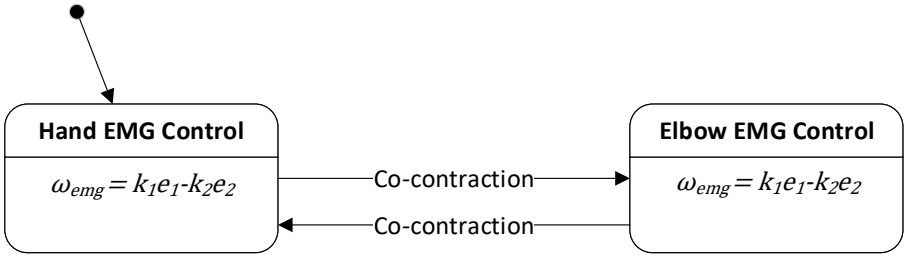

Fig. 19 conventional EMG control Finite State Machine

5.3.2 COMBINED IMU/EMG CONTROL

The combined IMU/EMG controller employs EMG in a similar manner to the conventional controller, but employs two additional components. First, an IMU is used to measure the angular velocity of the upper arm collinear with the elbow, which is used to command an elbow angular velocity equal and opposite to it, such that

$$\omega_{kin} = -\omega_{ua} \tag{6}$$

where ω_{kin} is the nominal kinematic coupling component of the elbow angular velocity command and ω_{ua} is the measured upper arm angular velocity. The coupling component essentially couples elbow extension to shoulder flexion, and thus provides an underlying or nominal kinematic synergy between the prosthetic elbow and intact shoulder joints. A video showing a subject wearing a prosthesis prototype and using the nominal kinematic coupling component of the controller (6) is shown in the supplemental material that accompanies this paper. This nominal coupling is supplemented with an EMG component of control, which is used exactly as it is in (2), although the resulting angular velocity is superposed onto the angular velocity associated with the kinematic coupling (6), such that the combined elbow angular velocity is:

$$\omega_{elb} = \omega_{kin} + \omega_{emg} \tag{7}$$

where ω_{elb} is the superposed elbow angular velocity command and ω_{emg} is the angular velocity command associated with the EMG. Thus, the coordinated controller is in implementation a relatively simple modification of the conventional EMG elbow controller, although rather than have the EMG command elbow velocity about a zero nominal angular velocity, it commands the elbow about a nominal kinematic coupling with the upper arm.

The second control component that distinguishes the combined IMU/EMG controller from the conventional EMG controller is the means by which the controller switches control between the elbow and hand. As in the conventional EMG controller, only one of the two components is controlled at any given time. Rather than use co-contraction to switch between the two, however, the IMU/EMG controller automatically switches control based on the measured motion of the hand, with respect to the inertial reference frame (IRF). Specifically, if the hand remains fixed relative to the IRF (for a brief period, approximately one sec), control automatically switches to the hand. If the hand moves relative to the IRF (above a minimum velocity), control automatically switches to the elbow. As such, the user must always initiate elbow movement with the shoulder. When the controller is in the elbow control state, the control equation is given by *(7)*. When the controller is in the hand control state, the control equation is the same as the conventional EMG controller, and is given by *(2)*. A state diagram of the combined IMU/EMG controller is shown in Fig. 20.

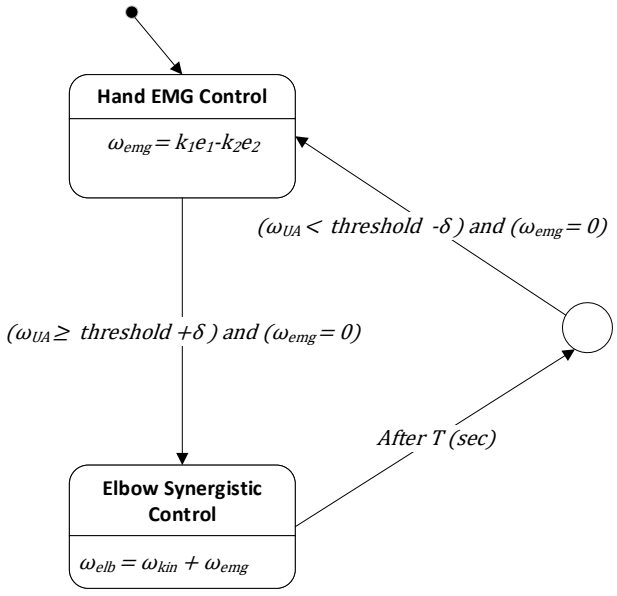

Fig. 20 Combined IMU/EMG Control

5.4 EXPERIMENTAL IMPLEMENTATION AND ASSESSMENT

The combined IMU/EMG control approach was implemented in a myoelectric transhumeral prosthesis prototype, and assessed in a set of experiments involving a single transhumeral amputee subject. Specifically, the ability of the subject to perform pick-and-place tasks was assessed when using the prosthesis prototype with the IMU/EMG controller, relative to her performance when using a conventional EMG controller.

5.4.1 MYOELECTRIC PROSTHESIS PROTOTYPE

The controller assessments were performed using a transhumeral prosthesis prototype, shown in Fig. 21 and previously described in [69], although for these experiments, the prosthesis was used with a powered wrist joint (i.e., consisted of a powered elbow and hand only). The hand prosthesis has been previously described in [11]. Although the hand is capable of multiple degrees of actuation, as used in this study the hand was limited to a single-degree-of-freedom power grasp.

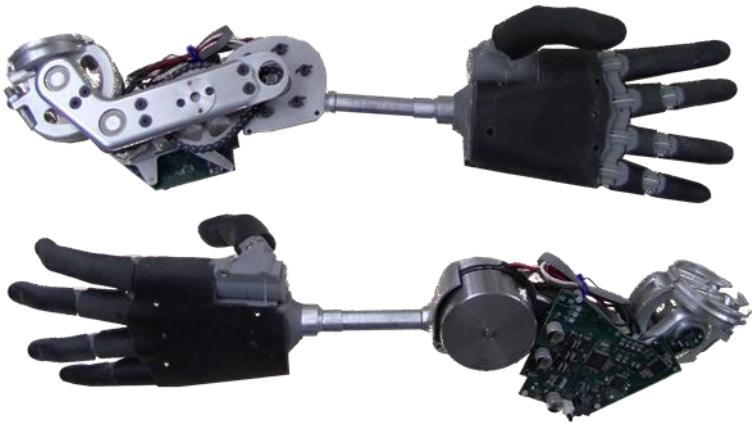

Fig. 21 Myoelectric hand and elbow prosthesis prototype

The essential characteristics of the arm are as follows. The elbow joint has a range of motion of 130 deg (15 deg to 145 deg flexion), and is capable of a maximum torque of 18 Nm and

maximum angular velocity of 80 deg/s. The hand is capable of a maximum grasp force of approximately 45 N and motion bandwidth of approximately 3 Hz. The elbow has a mass of 1050 g, and hand has a mass of 550 g (both including their respective embedded systems), such that the total prosthesis mass was 1.6 kg (not including the socket or battery). The prosthesis was powered by a 12 v, 2.9 Ah lithium ion battery pack consisting of three 18650 lithium ion cells, with a total mass of 145 g. For the experiments described here, the battery pack was placed on a table next to the experimental setup, in order to minimize the mass worn by the subject.

The embedded system on the arm includes: power conditioning circuitry; a brushless motor servo-amplifier and a PID controller for the elbow joint; an absolute encoder on the elbow joint; a 9-axis IMU (on the forearm); 8-channels of EMG signal conditioning (only two of which were used here); a CAN bus for communication with the embedded system in the hand, and for communication with a supervisory laptop computer. The embedded system in the hand includes four brushless motor servo-amplifiers – one for each brushless motor in the hand – and PID controllers for each. Although all control can be embedded on the arm, for purposes of the assessments conducted here, the arm was operated in a tethered mode of operation, in which sensor information from the embedded system (i.e., both EMG signals, joint position and velocity signals for the hand and elbow, and IMU measurements from the arm) were sent via the CAN bus to a laptop PC running Simulink with MATLAB Real-Time Windows Target, and hand or elbow motor position commands were sent back to the embedded system on the arm via the same CAN bus. Tethered operation facilitated controller development and implementation, as well as parameter adjustment and data acquisition. In order to provide an indication to the subject which component (hand or elbow) is active, an LED was affixed to the back of the hand and was illuminated when

the hand control was active, and was turned off otherwise. Similar visual indicators are often employed in commercial transhumeral myoelectric devices.

5.4.2 AMPUTEE SUBJECT

The subject was a left arm amputee, female, 40 years old. The subject was an experienced user of myoelectric transhumeral prostheses, although had no "daily-use" myoelectric prosthesis at the time the experiments were conducted. The prosthesis was affixed to the subject's residual limb via a standard socket and suspension sleeve.

5.4.3 EMG MEASUREMENT AND SIGNAL CONDITIONING

Disposable conductive-gel EMG electrodes (Rythmlink model DECUG10026) were positioned under the subject's socket, specifically on the anterior and posterior surfaces of the residual limb of the upper left arm with a reference electrode positioned proximal to the shoulder joint. The EMG leads were connected to the arm embedded system, where the differential signals were pre-amplified with a gain of 100 and digitally sampled using an EMG processing chip (Texas Instruments ADS1298), which also provided bandpass filtering (between 20 Hz and 500 Hz) and rectification. The rectified signal was sent via serial peripheral interface (SPI) to a PIC32 microcontroller (Microchip, Inc.), where it was low-pass-filtered at 5 Hz to provide an envelope of spatially integrated EMG activity. The (two) processed EMG signals were then streamed from the PIC32 via the CAN bus to the real-time environment provided by Simulink Real-Time Workshop (RTW).

5.4.4 EXPERIMENT SETUP AND PROTOCOL

The experimental assessments consisted of a series of pick-and-place tasks in which the subject was required to pick up a (tennis) ball resting on a table and place the ball into a target location inside one box of a four-box cabinet. The four-box cabinet was configured as a two-by-two box array, specifically two boxes across and two boxes high. Each box (or cell) measured approximately 25 cm wide by 17.5 cm high by 30 cm deep (10 in wide by 7 in high by 12 in deep), and each included a hole in the bottom, somewhat smaller in diameter than the tennis ball, to retain the ball when placed in it.

Experiments consisted of three sets of pick-and-place tasks, where each set required the subject to pick up the ball and place it in one of the four box locations. The order for each set of tasks was randomized. The subject completed three sets of the four pick-and-place tasks for each of the two controller types (i.e., twelve pick-and-place tasks per controller type). For each trial, the subject was required to stand with feet planted on a mat in front of a table, upon which the cabinet of boxes was located. The subject was required to start with her prosthetic arm by her side, with the elbow fully extended and hand open. For each pick-and-place task, the experimenter gave a start command and simultaneously started a timer, and subsequently stopped the timer when the ball was released from the hand and rested in the target box location (within the hole). Note that subject was required to complete each pick-and-place task fully – if the ball was dropped prior to placement in the box, the ball would be placed back at the starting position for the subject to re-attempt the task, until the task was successfully completed. Once the task was successfully completed, the ball was placed in the starting position, and the next target location (i.e., box location) was attempted. A photographic sequence of the subject performing the pick-and-place task with the prosthesis prototype is shown in Fig. 22.

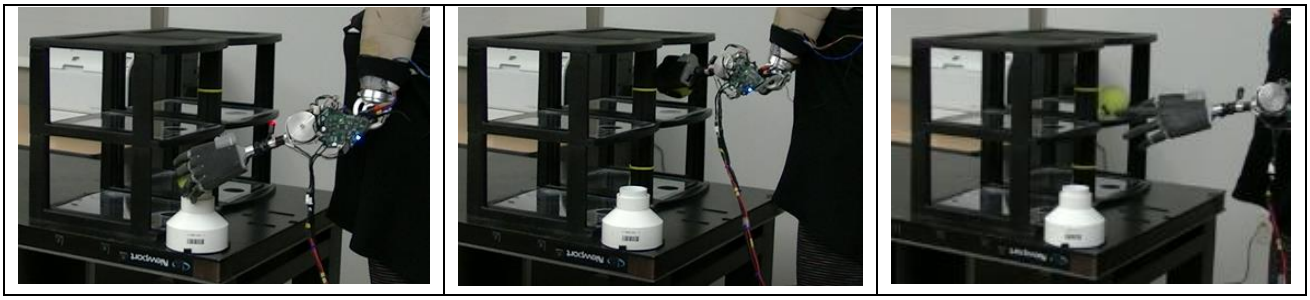

Fig. 22 Photographic sequence of subject performing pick-and-place task (box 4).

So that the subject could accommodate to each controller, the trials were conducted over a two consecutive days – first with the conventional EMG controller, and second with the combined IMU/EMG controller. On each day, an initial session was used to establish EMG thresholds and normalization gains, followed by an introduction to the control method, and a practice period during which the subject could practice controlling the elbow and hand, and could practice performing the pick-and-place tasks. The duration of the training/practice phase was generally between 15 and 30 min. Once sufficiently practiced, the subject performed a series of trials with the prescribed control approach, during which completion times associated with each of the pick-and-place tasks were recorded. Torso motion during the respective trials was also recorded, as subsequently described. The experimental protocol was approved by the Vanderbilt University Institutional Review Board.

5.4.5 MEASUREMENT OF TORSO MOTION

An IMU motion capture system was used to measure the extent of upper body movement required to complete the pick-and-place tasks. Specifically, an IMU motion capture (Xsens, MTw Awinda) was mounted on the chest of the subject via an elastic band, approximately at the xiphoid process. The torso IMU sent torso movement information wirelessly to a Bluetooth receiver which is connected to a laptop station via a USB cable. The torso data were recorded using the software associated with the IMU motion capture system (Xsens, MVN Studio).

5.5 RESULTS

The efficacy of the combined EMG/IMU controller in enabling the previously described pick-and-place tasks, relative to the conventional EMG controller, was assessed by the relative average time required to perform the tasks with one controller, relative to the other. Torso motion of the subject was also measured during the tasks, to assess the relative extent of compensatory torso motion when using the two controllers. Note that the subject was required to stand in place during the tasks, so that all compensatory body motion employed during the tasks should be captured by torso movement. A video showing trials from the experiments of both the controllers is provided in the supplementary material.

The data representing the task completion times each task and each trial, along with the average times and standard deviations for each box location and each iteration, are given in Table V and Table VI for the conventional EMG controller and the combined EMG/IMU controller, respectively. As shown in Table V, for Iteration 2, Box 2 using the conventional EMG controller, the subject dropped the ball several times, and therefore required 1 min and 46 sec (106 sec) to complete the task. Since this time was not representative of the other times for that box location and controller (which were 30.4 and 26.4 sec, respectively), and since it was likely a result of insufficient practice with the controller and prosthesis prototype, the authors omitted this data point from the average. Specifically, rather than use the average and standard deviation resulting from the three trials – 54.4 sec and 45 sec, respectively – the authors used instead only the average of the two representative trials – which was 28.4 sec and 2.87 sec, respectively. These values are shown in Table V within brackets in the average and standard deviation columns. Thus, the outlying data point was excluded from all comparative assessment of the two controllers. This data is summarized in Fig. 23, which shows the completion time averages and standard deviations for

each controller (excluding the outlying data point). As summarized in the tables, the overall average completion time for the conventional EMG controller was 21.5 sec, and was 10.8 sec for the combined EMG/IMU controller. As such, the subject was able to complete the pick-and-place tasks on average approximately 50% faster with the combined controller. As indicated by the bar chart, the performance advantage was roughly consistent across box locations. Paired t-tests assessing significant differences in means between the two controllers for each box location, and for the overall average completion times, indicated that the differences in means for boxes 2 and 3 were significant at 5% confidence levels, while the differences in means for boxes 1 and 4 were significant at approximately 15% confidence levels.

Table V

Completion times for all trials for the conventional EMG controller

	Iteration 1 (sec)	**Iteration 2 (sec)**	**Iteration 3 (sec)**	**Average (sec)**	**Std. Dev.**
Box 1	31.6	16.0	21.5	23.0	7.9
Box 2	30.4	106.3	26.4	54.4 [28.4]	45.0 [2.9]
Box 3	14.0	17.4	22.0	17.8	4.0
Box 4	20.8	15.4	13.7	16.6	3.7
Average	24.2	16.3	20.9	21.5	4.6

Table VI

Completion times for all trials for the combined EMG/IMU controller

	Iteration 1 (sec)	**Iteration 2 (sec)**	**Iteration 3 (sec)**	**Average (sec)**	**Std. Dev.**
Box 1	7.7	12.9	17.7	12.7	5.0
Box 2	8.2	6.4	11.4	8.7	2.5
Box 3	8.6	10.8	9.6	9.7	1.1
Box 4	9.2	13.9	13.7	12.3	2.7
Average	8.4	11.0	13.1	10.8	2.8

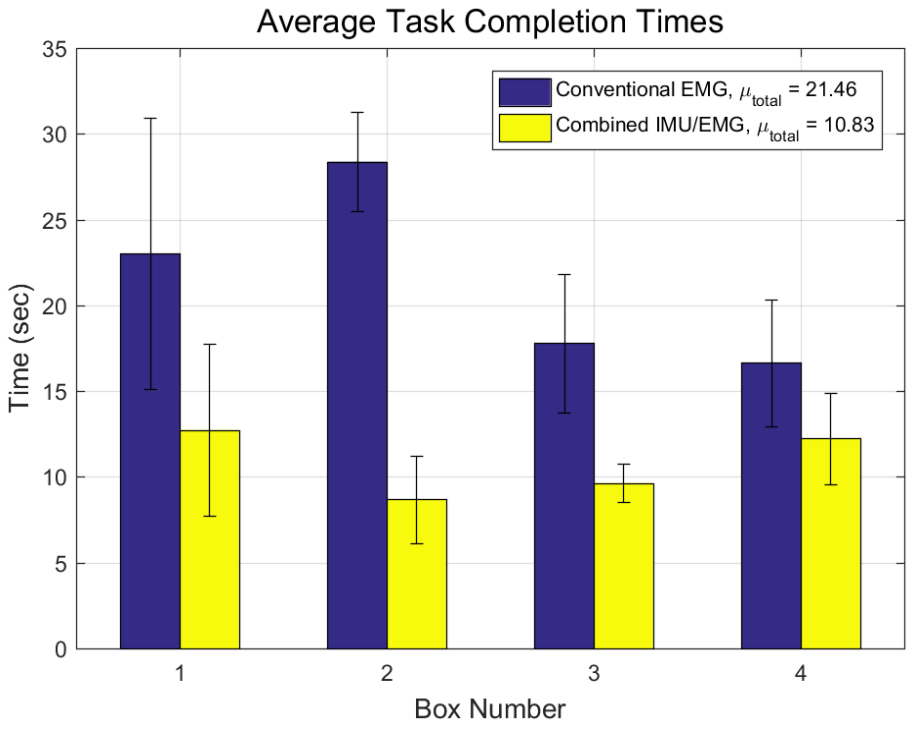

Fig. 23 Average task completion times across all trials, corresponding to each respective target box location, representing a variety of reaching movements

Torso motion was measured during all pick-and-place tasks, in order to ensure that the performance difference was not a result of substantive changes in compensatory torso motion. Specifically, the torso angles, with respect to the vertical, in the sagittal and coronal planes were recorded at the time each reaching task was completed (i.e., when the ball was successfully released in the target box). These measurements in effect characterized the torso configuration upon completion of each reaching task, and specifically how much forward and sideways lean was employed to reach a given target location. The magnitude of respective torso angles, averaged for each target location and each controller type, are shown in Fig. 24 and Fig. 25, respectively, along with error bars indicating plus and minus one standard deviation for each. Paired t-tests assessing significant differences in means of torso angles between controllers indicate that no significant differences exist between torso motion means for any of the trials at a 5% confidence level.

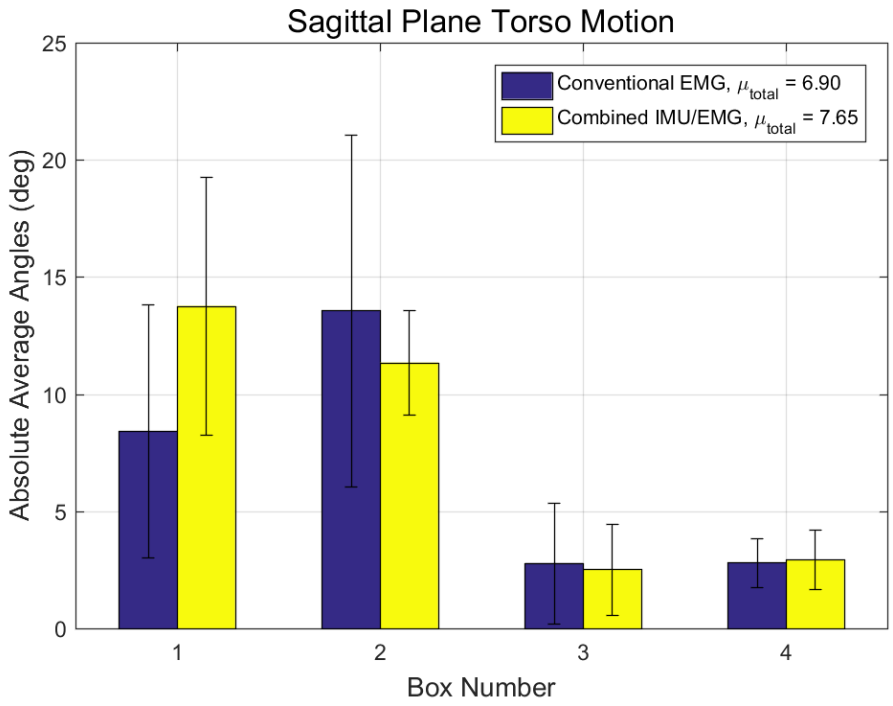

Fig. 24 Comparison of the torso motion in the sagittal plane

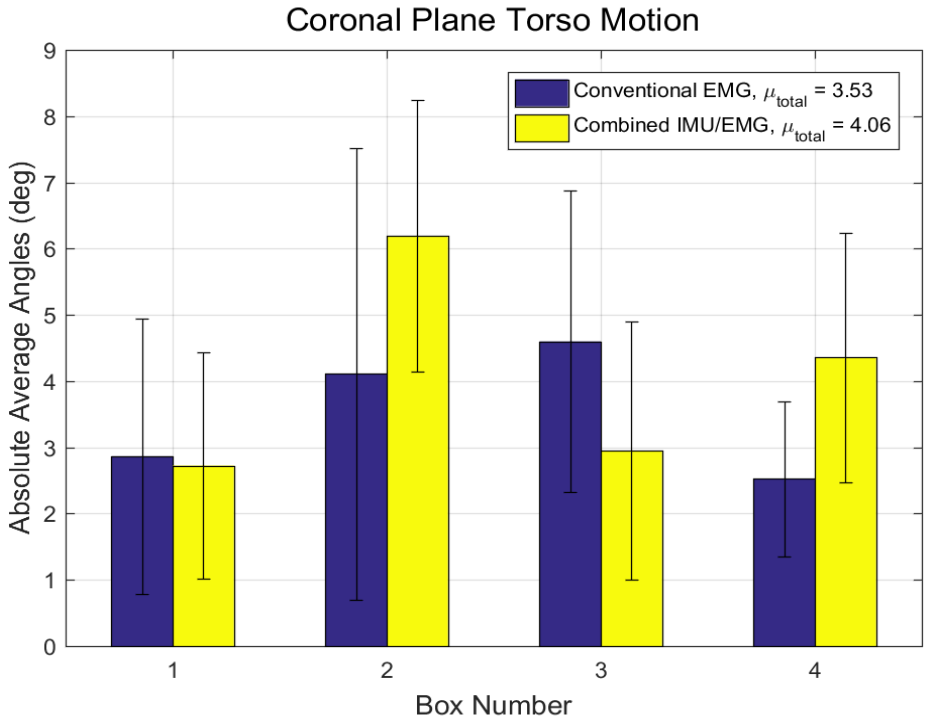

Fig. 25 Comparison of the torso motion in the sagittal plane

5.6 DISCUSSION

Fig. 23 through Fig. 25 indicate that the combined EMG/IMU controller enabled an average of approximately 50% faster completion times, without necessitating additional compensatory torso motion relative to the conventional EMG control.

5.6.1 REPRESENTATIVE DATA

Fig. 26 and Fig. 27 show controller data during performance of a representative pick-and-place task (i.e., while picking and placing the ball into box number 3) using the conventional EMG controller (Fig. 26) and the combined EMG/IMU controller (Fig. 27), respectively. Specifically, Fig. 26 shows the elbow EMG command for the conventional EMG controller over the task performance period, where the gray bands indicate periods of hand control and the white bands indicate periods of elbow control. The periods of activity correspond to positioning the elbow to pick up the ball, grasping the ball, adjusting the elbow by either flexing or extending (and flexing the shoulder) to place the ball, and releasing the ball. One can note the co-contraction “spikes” in the EMG signals that separate the period of hand and elbow control.

Fig. 27 shows the corresponding controller data during the same pick-and-place task (i.e., box number 3), while using the combined EMG/IMU controller, showing both the IMU component of elbow angular velocity *(6)* and the EMG component (2), over the entire task performance period. The total elbow angular velocity command (7) is the direct sum of these components. The gray bands in Fig. 27 indicate periods of hand control and the white bands indicate periods of elbow control. Note that co-contraction is not present at the transitions between elbow and hand control, since it is not used in the coordinated controller. As shown in the figure, the subject employs both components when controlling the elbow during the task.

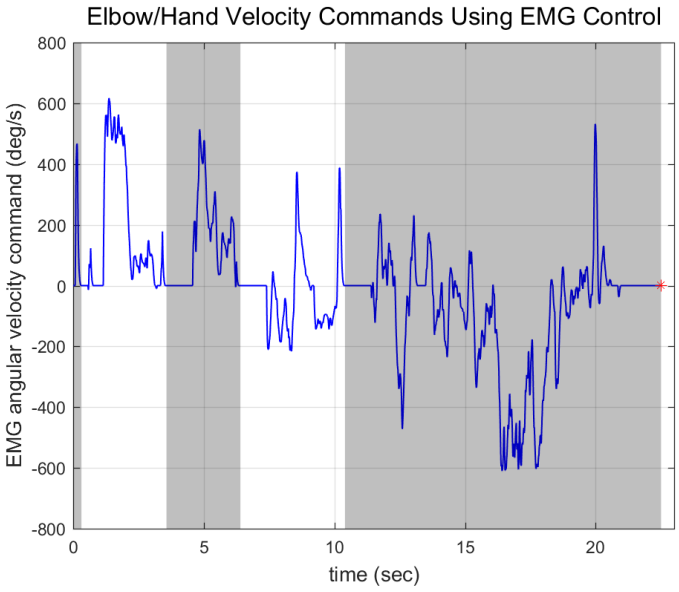

Fig. 26 Elbow commands during a representative pick-and-place task (box no. 1) performed with the sequential EMG controller. The gray bands indicate the periods of hand control, while the white bands indicate the periods of elbow control. Positive and negative elbow commands indicate elbow flexion and extension respectively.

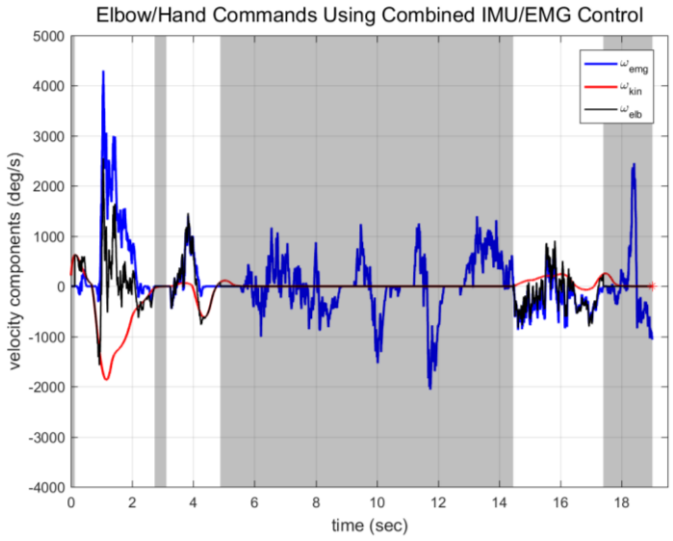

Fig. 27 EMG and IMU elbow angular position commands during a representative pick-and-place task (box no. 1) performed with the coordinated controller. The gray bands indicate the periods of hand control, while the white bands indicate the periods of elbow control. Positive elbow angular position commands indicate flexion while negative commands indicate extension

5.6.2 LIMITATIONS

The intent of this paper was to assess the extent to which supplementing EMG input from a user with movement information about the residual limb, provided by an IMU, could potentially improve prosthesis control. The experiments performed here appear to indicate that the added control information can improve prosthesis control, although the work has a number of limitations. First, the assessments involved only a single amputee subject. The authors found that locating transhumeral amputee subjects with appropriate range of shoulder motion and good EMG sites is challenging, but nonetheless, these assessments should be performed on multiple subjects to better assess the potential value of the proposed combined control approach. Second, this assessment entailed only pick-and-place tasks. In order to vary the geometry of the pick-and-place tasks, the authors used multiple box locations. Nonetheless, it's not clear how the underlying kinematic coupling between the upper arm and elbow joint would affect other activities of daily living (ADLs). Conducting assessments employing a more complete set of tasks would provide valuable information regarding the extent to which the proposed coupling either enhances or impairs the conduct of other ADLs.

Another limitation of this work is that, since the two control components (kinematic coupling and motion-based state-switching) were not separately assessed, it's difficult to assess the relative value of each. Data (such as that shown in Fig. 27) shows that the subject employed both components, but without conducting experiments that separate the two components, the relative value of each cannot be fully assessed.

A limitation of the controller is that both the biceps and triceps brachii span the shoulder joint. As such, shoulder movement results in muscular contraction. This is the case for both the

conventional and the combined controllers. Shoulder flexion generally results in biceps EMG, which provides a flexive angular velocity at the elbow, as given by *(2)*. The same shoulder flexion, however, results in an elbow extension command associated with the kinematic coupling component *(6)*. As such, these two components can cancel each other if signal conditioning is not appropriately configured. This tendency to cancel can be seen in the two angular velocity control components shown in Fig. 27. In order to avoid such cancellation, the thresholds associated with EMG control were increased for the combined EMG/IMU controller, so that the low-amplitude EMG associated with shoulder flexion would not cancel the component provided by the kinematic coupling.

5.6.3 GENERAL COMMENTS

One of the major challenges in the control of myoelectric prostheses, and transhumeral myoelectric prostheses in particular, is the extremely limited amount of control information by which the user can communication volitional intent to the device. In the case of a transhumeral prosthesis, a user must control multiple components with limited control information, typically with a single channel of (agonist/antagonist) EMG. The movement of the residual limb potentially offers a considerably amount of addition control information, specifically with regard to shoulder motion, which is directly associated with the user's neuromuscular and musculoskeletal system. This information is readily measured in a repeatable, reliable, high-bandwidth, low-noise manner via an IMU, which is easily added onto a myoelectric prosthesis. Based on the limited study presented here, this information can substantially improve performance during the tasks performed in this assessment. The authors believe the measurement of residual limb motion could be further exploited by measuring movement in multiple planes of motion (i.e., motion was generally measured in a single plane in this work, at least with respect to the kinematic coupling component),

and also potentially by using measured residual limb motion with other control methodologies, such as pattern recognition methodologies, which would presumably complement such approaches and increase their efficacy, relative to using EMG alone.

5.7 CONCLUSION

The authors conducted a limited investigation on the value of incorporating residual limb motion into the control of a transhumeral myoelectric prosthesis. Specifically, an IMU on a prosthesis prototype was employed to measure the motion of the upper arm, and was in turn used to modify a conventional EMG controller in two ways: 1) a nominal kinematic coupling was implemented at the elbow joint, upon which standard EMG control was superposed; and 2) the control was automatically switched to the hand when the hand was essentially motionless relative to an inertial reference frame. The control approach was implemented on a transhumeral prosthesis prototype, and functional assessments were performed on a single amputee subject, indicating that the subject was able to perform a series of pick-and-place tasks 50% faster when the controller was supplemented with information from the IMU. Although the work has several limitations, the authors believe the use of an IMU to supplement control information has real promise in improving the control of myoelectric prostheses, both with the control method proposed, and by supplementing other proposed control methods with IMU measurements.

CHAPTER 6

CONCLUSION

This dissertation has presented a control method and assessment of an upper extremity prosthetic system. Through the process of many design iterations, the combined IMU/EMG control method was shown to enhance the conduct of activities of daily living involving reaching tasks. In addition, the combined IMU/EMG control method delivered an intuitive control relative to the commercially available devices and a simple control method relative to the recent research prosthetic control methods. The combined IMU/EMG control method was assessed by healthy subjects using a virtual environment and by amputee using a transhumeral prosthesis prototype to assess the performance of the controller in real-world applications. Finally, the novel controller presented in this work represents a convenient testbed for the development of additional novel upper limb controllers, which will enhance the capabilities of amputees.

6.1 FUTURE WORK

The controller presented in this work is one of the first controllers that coordinates between arm joints intuitively. However, further fine tuning of this controller should be considered in future work. Specifically, fine tuning the EMG signals while flexing the shoulder joint as described in the limitation section in chapter VI. The use of the IMU has enabled coordination between arm joints and therefore examining the control of additional arm joints, such as a wrist, should also be investigated. While the current prosthesis prototype has provided convenient testbed, experiments indicated that the weight of the prosthesis should be decreased, and therefore a lighter prototype design should be taken into consideration in future work.

REFERENCES

[1] S. A. Dalley, T. E. Wiste, T. J. Withrow, and M. Goldfarb, "Design of a Multifunctional Anthropomorphic Prosthetic Hand With Extrinsic Actuation," *IEEE/ASME Transactions on Mechatronics*, vol. 14, pp. 699-706, 2009.

[2] S. A. Dalley, T. E. Wiste, H. A. Varol, and M. Goldfarb, "A Multigrasp Hand Prosthesis for Transradial Amputees," in *IEEE International Conference of the Engineering in Medicine and Biology Society*, Buenos Aires, Argentina, 2010, pp. 5062-5065.

[3] S. A. Dalley, H. A. Varol, and M. Goldfarb, "Continuous Position and Force Control of a Multigrasp Myoelectric Transradial Prosthesis," in *Myoelectric Controls/Powered Prosthetics Symposium (MEC)*, Fredericton, Canada, 2011, pp. 79-81.

[4] S. Dalley, H. Varol, and M. Goldfarb, "Multigrasp Myoelectric Control for a Transradial Prosthesis," in *IEEE International Conference on Rehabilitiation Robotics*, Zurich, Switzerland, 2011, pp. 1-6.

[5] S. A. Dalley, Varol, H. A., Goldfarb, M, "A Method for the Control of Multigrasp Myoelectric Prosthetic Hands," *IEEE Transactions on Neural Systems and Rehabilitation Engineering*, vol. 20, pp. 58-67, 2012.

[6] N. A. Alshammary, S. A. Dalley, and M. Goldfarb, "Assessment of a multigrasp myoelectric control approach for use by transhumeral amputees," in *IEEE International Conference of the Engineering in Medicine and Biology Society*, 2012, pp. 968-971.

[7] D. A. Bennett, S. A. Dalley, and M. Goldfarb, "Design of a hand prosthesis with precision and conformal grasp capability," in *IEEE International Conference of the Engineering in Medicine and Biology Society*, 2012, pp. 3044-3047.

[8] S. A. Dalley, D. A. Bennett, and M. Goldfarb, "Preliminary functional assessment of a multigrasp myoelectric prosthesis," in *IEEE International Conference of the Engineering in Medicine and Biology Society*, 2012, pp. 4172-4175.

[9] S. A. Dalley, D. A. Bennett, and M. Goldfarb, "Functional assessment of a Multigrasp Myoelectric prosthesis: An amputee case study," in *IEEE International Conference on Robotics and Automation*, Karlsruhe, Germany, 2013, pp. 2640-2644.

[10] S. A. Dalley, D. A. Bennett, and M. Goldfarb, "Functional assessment of the vanderbilt multigrasp myoelectric hand: A continuing case study," in *IEEE International Conference of the Engineering in Medicine and Biology Society*, Chicago, IL, 2014, pp. 6195-6198.

[11] D. A. Bennett, S. A. Dalley, D. Truex, and M. Goldfarb, "A Multigrasp Hand Prosthesis for Providing Precision and Conformal Grasps," *IEEE/ASME Transactions on Mechatronics*, vol. 20, pp. 1697-1704, 2015.

[12] K. A. Raichle, "Prosthesis use in persons with lower- and upper-limb amputation," *The Journal of Rehabilitation Research and Development,* vol. 45, pp. 961-972, 2008.

[13] K. Ziegler-Graham, E. Mackenzie, P. Ephraim, T. Travison, and R. Brookmeyer, "Estimating the Prevalence of Limb Loss in the United States: 2005 to 2050," *Archives of Physical Medicine and Rehabilitation,* vol. 89, pp. 422-429, 2008.

[14] NLLIC-Staff, "Amputation Statistics by Cause: Limb Loss in the United States," National Limb Loss Information Center, Fact Sheet,2008.

[15] J. A. Doubler and D. S. Childress, "An analysis of extended physiological proprioception as a prosthesis-control technique," *J Rehabil Res Dev,* vol. 21, pp. 5-18, May 1984.

[16] P. J. Kyberd, D. J. Beard, J. J. Davey, and J. D. Morrison, "A Survey of Upper-Limb Prosthesis Users in Oxfordshire," *Journal of Prosthetics and Orthotics,* vol. 10, pp. 85-91, 1998.

[17] D. J. Atkins, D. C. Y. Heard, and W. H. Donovan, "Epidemiological overview of individuals with upper-limb loss and their reported research priorities," *Journal of Prosthetics and Orthotics,* vol. 8, pp. 2-10, 1996.

[18] D. J. H. Atkins, D. C. Y.Donovan, W. H., "Epidemiological overview of individuals with upper-limb loss and their reported research priorities," *Journal of Prosthetics and Orthotics,* vol. 8, pp. 2-10, 1996.

[19] M. Popovic and D. Popovic, "Cloning biological synergies improves control of elbow neuroprostheses," *Engineering in Medicine and Biology Magazine, IEEE,* vol. 20, pp. 74-81, 2001.

[20] S. G. Millstein, Heger, H.,Hunter, G. A., "Prosthetic use in adult upper limb amputees: a comparison of the body powered and electrically powered prostheses," *Prosthetics and Orthotics International,* vol. 10, pp. 27-34, 1986.

[21] R. B. Stein, Walley, M., "Functional comparison of upper extremity amputees using myoelectric and conventional prostheses," *Arch Phys Med Rehabil,* vol. 64, pp. 243-8, Jun 1983.

[22] T. E. Wiste, S. A. Dalley, H. A. Varol, and M. Goldfarb, "Design of a Multigrasp Transradial Prosthesis," *ASME Journal of Medical Devices,* vol. 5, pp. 1-7, 2011.

[23] J. T. Belter, J. L. Segil, A. M. Dollar, and R. F. Weir, "Mechanical design and performance specifications of anthropomorphic prosthetic hands: A review," *Journal of Rehabilitation Research and Development,* vol. 50, p. 20, 2013.

[24] Y. Kamikawa and T. Maeno, "Underactuated five-finger prosthetic hand inspired by grasping force distribution of humans," in *Intelligent Robots and Systems, 2008. IROS 2008. IEEE/RSJ International Conference on*, 2008, pp. 717-722.

[25] T. Lenzi, J. Lipsey, and J. W. Sensinger, "The RIC Arm—A Small Anthropomorphic Transhumeral Prosthesis," *IEEE/ASME Transactions on Mechatronics,* vol. 21, pp. 2660-2671, 2016.

[26] L. Resnik, S. L. Klinger, and K. Etter, "The DEKA Arm: Its features, functionality, and evolution during the Veterans Affairs Study to optimize the DEKA Arm," *Prosthetics and Orthotics International,* vol. 38, pp. 492-504, 2014.

[27] J. Davidson, "A survey of the satisfaction of upper limb amputees with their prostheses, their lifestyles, and their abilities," *J Hand Ther,* vol. 15, pp. 62-70, Jan-Mar 2002.

[28] A. Z. Escudero, J. Alvarez, and L. Leija, "Development of a parallel myoelectric prosthesis for above elbow replacement," in *Proceedings of the Second Joint 24th Annual Conference and the Annual Fall Meeting of the Biomedical Engineering Society] [Engineering in Medicine and Biology*, 2002, pp. 2404-2405 vol.3.

[29] L. V. McFarland, Hubbard Winkler, S. L.,Heinemann, A. W.,Jones, M.,Esquenazi, A., "Unilateral upper-limb loss: satisfaction and prosthetic-device use in veterans and servicemembers from Vietnam and OIF/OEF conflicts," *Journal of Rehabilitation Research and Development,* vol. 47, pp. 299-316, 2010.

[30] S. D. Iftime, L. L. Egsgaard, and M. B. Popovic, "Automatic determination of synergies by radial basis function artificial neural networks for the control of a neural prosthesis," *Neural Systems and Rehabilitation Engineering, IEEE Transactions on,* vol. 13, pp. 482-489, 2005.

[31] M. P. alexander Boschmann, Michael Robrecht,Martin Hahn,Michael Winkler, "Development of a Pattern Recognition-Based Myoelectric Transhumeral Prosthesis With Multifunctional Simultaneous Control Using A Model-Driven Approach for Mechatronic System," 2011.

[32] L. Hargrove, Losier, Y.,Lock, B.,Englehart, K.,Hudgins, B., "A real-time pattern recognition based myoelectric control usability study implemented in a virtual environment," in *IEEE International Conference of the Engineering in Medicine and Biology Society*, 2007, pp. 4842-4845.

[33] E. Scheme, Englehart, K., "Electromyogram pattern recognition for control of powered upper-limb prostheses: State of the art and challenges for clinical use," *Journal of Rehabilitation Research and Development,* vol. 48, p. 16, 2011.

[34] T. U. Eiichi Inohira, Hirokazu Yokoi, "Generalization Capability of Neural Networks For Generation Of Coordinated Motion Of A hybrid Prosthesis With A Healthy Arm," *International Journal of Innovative Computing, Information and Control,* vol. 4, p. 13, 2008.

[35] M. Asghari Oskoei and H. Hu, "Myoelectric control systems--A survey," *Biomedical Signal Processing and Control,* vol. 2, pp. 275-294, 2007.

[36] L. Miller, R. Lipschutz, K. Stubblefield, B. Lock, H. Huang, T. Williamsiii, *et al.*, "Control of a Six Degree of Freedom Prosthetic Arm After Targeted Muscle Reinnervation Surgery," *Archives of Physical Medicine and Rehabilitation,* vol. 89, pp. 2057-2065, 2008.

[37] T. A. Kuiken, G. Li, B. A. Lock, and et al., "Targeted muscle reinnervation for real-time myoelectric control of multifunction artificial arms," *JAMA,* vol. 301, pp. 619-628, 2009.

[38] J. T. Belter and A. M. Dollar, "Performance characteristics of anthropomorphic prosthetic hands," in *Rehabilitation Robotics (ICORR), 2011 IEEE International Conference on*, 2011, pp. 1-7.

[39] M. Vuskovic and D. Sijiang, "Classification of prehensile EMG patterns with simplified fuzzy ARTMAP networks," in *Proceedings of the 2002 International Joint Conference on Neural Networks*, 2002, pp. 2539-2544.

[40] J. Zhao, Z. Xie, L. Jiang, H. Cai, H. Liu, and G. Hirzinger, "EMG control for a five-fingered underactuated prosthetic hand based on wavelet transform and sample entropy," in *IEEE/RSJ International Conference on Intelligent Robots and Systems*, 2006, pp. 3215-3220.

[41] L. Hargrove, Y. Losier, B. Lock, K. Englehart, and B. Hudgins, "A real-time pattern recognition based myoelectric control usability study implemented in a virtual environment," in *IEEE International Conference of the Engineering in Medicine and Biology Society*, 2007, pp. 4842-4845.

[42] G. Li, A. E. Schultz, and T. A. Kuiken, "Quantifying pattern recognition-based myoelectric control of multifunctional transradial prostheses," *IEEE Transactions on Neural Systems and Rehabilitation Engineering*, vol. 18, pp. 185-192, 2010.

[43] P. H. Chappell and P. J. Kyberd, "Prehensile control of a hand prosthesis by a microcontroller," *Journal of Biomedical Engineering*, vol. 13, pp. 363-369, 1991.

[44] P. J. Kyberd, N. Mustapha, F. Carnegie, and P. H. Chappell, "A clinical experience with a hierarchically controlled myoelectric hand prosthesis with vibro-tactile feedback," *Prosthet Orthot Int*, vol. 17, pp. 56-64, Apr 1993.

[45] P. J. Kyberd, O. E. Holland, P. H. Chappell, S. Smith, R. Tregidgo, P. J. Bagwell, *et al.*, "MARCUS: a two degree of freedom hand prosthesis with hierarchical grip control," *IEEE Transactions on Rehabilitation Engineering*, vol. 3, pp. 70-76, 1995.

[46] C. M. Light, P. H. Chappell, B. Hudgins, and K. Englehart, "Intelligent multifunction myoelectric control of hand prostheses," *Journal of Medical Engineering & Technology*, vol. 26, pp. 139-146, 2002.

[47] D. P. J. Cotton, A. Cranny, P. H. Chappell, N. M. White, and S. P. Beeby, "Control strategies for a multiple degree of freedom prosthetic hand," *Measurement & Control*, vol. 40, pp. 24-27, Feb 2007.

[48] C. Cipriani, F. Zaccone, S. Micera, and M. C. Carrozza, "On the shared control of an EMG-controlled prosthetic hand: analysis of user-prosthesis interaction," *IEEE Transactions on Robotics*, vol. 24, pp. 170-184, 2008.

[49] S. A. Dalley, H. A. Varol, and M. Goldfarb, "A method for the control of multigrasp myoelectric prosthetic hands," *IEEE Transactions on Neural Systems and Rehabilitation Engineering*, vol. 20, pp. 58-67, 2012.

[50] D. R. Kaliki RK, Loeb GE, "Prediction of Distal Arm Posture From Shoulder Posture During Three-Dimensional Reaching," in *12th Annual Conference of the International Functional Electrical Stimulation Society*, ed. Shriners Hospital for Children, Philadelphia, PA, USA: IFESS_2007, 2007.

[51] R. R. Kaliki, R. Davoodi, and G. E. Loeb, "Prediction of Distal Arm Posture in 3-D Space From Shoulder Movements for Control of Upper Limb Prostheses," *Proceedings of the IEEE,* vol. 96, pp. 1217-1225, 2008.

[52] S. D. Iftime, L. L. Egsgaard, and M. B. Popovic, "Automatic determination of synergies by radial basis function artificial neural networks for the control of a neural prosthesis," *IEEE Transactions on Neural Systems and Rehabilitation Engineering,* vol. 13, pp. 482-489, 2005.

[53] D. B. Popovic, M. B. Popovic, and T. Sinkjasr, "Life-like Control for Neural Prostheses: "Proximal Controls Distal"," in *Engineering in Medicine and Biology Society, 2005. IEEE-EMBS 2005. 27th Annual International Conference of the*, 2005, pp. 7648-7651.

[54] D. Popovic and M. Popovic, "Tuning of a nonanalytical hierarchical control system for reaching with FES," *Biomedical Engineering, IEEE Transactions on,* vol. 45, pp. 203-212, 1998.

[55] M. Popovic and D. Popovic, "Synergistic control for an elbow neuroprosthesis," *A A,* vol. 10, p. 5, 2000.

[56] L. Cenciotti, S. Micera, M. Carrozza, P. Dario, and M. Popovic, "A hybrid system for the prediction of upper arm articular synergies using statistical and soft-computing techniques," in *Proc of the Sixth Annual IFESS Conf IFESS*, 2001, pp. 253-5.

[57] C. Lauretti, A. Davalli, R. Sacchetti, E. Guglielmelli, and L. Zollo, "Fusion of M-IMU and EMG signals for the control of trans-humeral prostheses," in *2016 6th IEEE International Conference on Biomedical Robotics and Biomechatronics (BioRob)*, 2016, pp. 1123-1128.

[58] S. M. Ning Jiang; Dosen, K.; Farina, D. (2012, Sept. 2012) Myoelectric Control of Artificial Limbs—Is There a Need to Change Focus? *in Signal Processing Magazine*. 152 -150.

[59] E. Biddiss, D. Beaton, and T. Chau, "Consumer design priorities for upper limb prosthetics," *Disability & Rehabilitation: Assistive Technology,* vol. 2, pp. 346-357, 2007.

[60] E. A. Biddiss and T. T. Chau, "Upper limb prosthesis use and abandonment: a survey of the last 25 years," *Prosthet Orthot Int,* vol. 31, pp. 236-57, Sep 2007.

[61] E. Scheme and K. Englehart, "Electromyogram pattern recognition for control of powered upper-limb prostheses: State of the art and challenges for clinical use," *Journal of Rehabilitation Research and Development,* vol. 48, p. 16, 2011.

[62] a. Boschmann, M. Platzner, M. Robrecht, M. Hahn, and M. Winkler, "Development of a Pattern Recognition-Based Myoelectric Transhumeral Prosthesis With Multifunctional Simultaneous Control Using A Model-Driven Approach for Mechatronic System," 2011.

[63] B. A. Lock, K. Englehart, and B. Hudgins, "Real-Time Myoelectric Control in A Virtual Environment to Relate usability Vs. Accuracy," 2005.

[64] E. Inohira, T. Uoi, and H. Yokoi, "Generalization Capability of Neural Networks For Generation Of Coordinated Motion Of A hybrid Prosthesis With A Healthy Arm," *International Journal of Innovative Computing, Information and Control*, vol. 4, p. 13, 2008.

[65] C. sherstan, J. Modayil, and P. M. Pilarski, "A collaborative Approach to the simultaneous Multi-joint control of A ProstheticArm," 2015.

[66] M. R. Tucker, J. Olivier, A. Pagel, H. Bleuler, M. Bouri, O. Lambercy, *et al.*, "Control strategies for active lower extremity prosthetics and orthotics: a review," *Journal of NeuroEngineering and Rehabilitation*, vol. 12, p. 1, 2015.

[67] M. Merad, A. Roby-Brami, and N. Jarrassé, "Towards the implementation of natural prosthetic elbow motion using upper limb joint coordination," in *2016 6th IEEE International Conference on Biomedical Robotics and Biomechatronics (BioRob)*, 2016, pp. 821-826.

[68] M. Merad, M. É. de, A. Roby-Brami, and N. Jarrassé, "Intuitive prosthetic control using upper limb inter-joint coordinations and IMU-based shoulder angles measurement: A pilot study," in *2016 IEEE/RSJ International Conference on Intelligent Robots and Systems (IROS)*, 2016, pp. 5677-5682.

[69] D. A. Bennett, J. E. Mitchell, D. Truex, and M. Goldfarb, "Design of a Myoelectric Transhumeral Prosthesis," *IEEE/ASME Transactions on Mechatronics*, vol. 21, pp. 1868-1879, 2016.